Design, mechanical performance and deformation characteristics of a new γ' strengthened Ni-based superalloy with high-entropy matrix

Martin Detrois[1,2], Paul D. Jablonski[1], Stoichko Antonov[3,4], Sammy Tin[4], Jeffrey A. Hawk[1]

[1]National Energy Technology Laboratory, Albany OR, USA

[2]LRST, Pittsburgh PA, USA

[3]University of Science and Technology, Beijing, China

[4]Illinois Institute of Technology, Chicago IL, USA

Introduction

Superalloys and HEAs

Design approach for multiple property optimization

- Ni-based superalloys for high-temperature applications, alloying used for:
  - γ' strengthening, controlled with Al, Ti, Nb
  - Anti-phase boundary energy, stacking fault energy
  - Solid-solution strengthening (Mo, W, …)
  - Lattice misfit
  - Grain boundaries (C, B, …)
- HEA
  - Recent approaches show γ' strengthening and investigation of grain boundary phases, high-entropy superalloys… => distance from single solid-solution phase, near equiatomic

$$\Delta S_{conf} \geq 1.5R \qquad \Delta S_{conf} = -R\sum_i x_i ln_{x_i}$$

T.-K. Tsao, A.-C. Yeh, C.-M. Kuo, K. Kakehi, H. Murakami, J.-W. Yeh, S.-R. Jian, The High Temperature Tensile and Creep Behaviors of High Entropy Superalloy, Sci. Rep. 7 (2017) 12658

Configurational entropy of some Ni-based superalloys

Alloy	ΔS_{conf}
> 1.5R	
LSHR	1.51R
< 1.5R	
Haynes R-41	1.498R
Rene 104	1.48R
Alloy 10	1.44R
Nimonic 105	1.37R
Udimet 720	1.36R
Hastelloy X	1.30R
Inconel 740	1.30R
Waspaloy	1.25R
Incoloy 909	1.18R
ME3	1.08R
Inconel 718	0.85R

Concept

ASC Alloys

- Instead of starting with a high-entropy alloy, a Ni-based superalloy is designed using the entropy concept only for the γ matrix
- Consider γ' strengthening, misfit, carbides, phase stability, potential oxidation resistance first
- Consider the entropy of the matrix (γ) as a function of temperature

$$\Delta S_{conf(matrix)} > 1.5R$$

Configurational entropy of the ASC alloys calculated based on their overall composition (ΔS_{conf})

Alloy	ΔS_{conf}
> 1.5R	
ASC3	1.57R
ASC2	1.56R
ASC1	1.53R

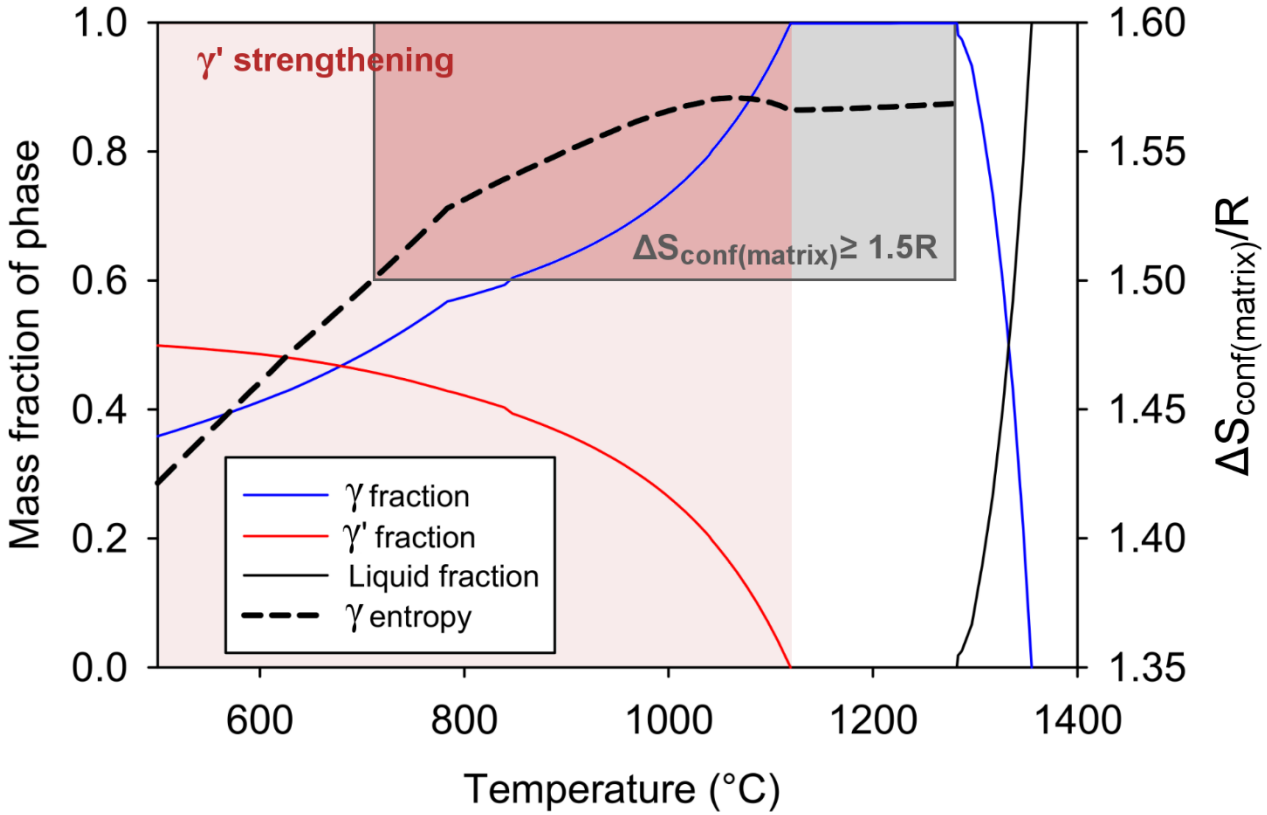

Predicted property diagram for ASC3 showing selected phases (γ matrix, γ' and liquid) with added curve for the calculated configurational entropy of the γ matrix ($\Delta S_{conf(matrix)}$)

Concept

Thermodynamic Predictions

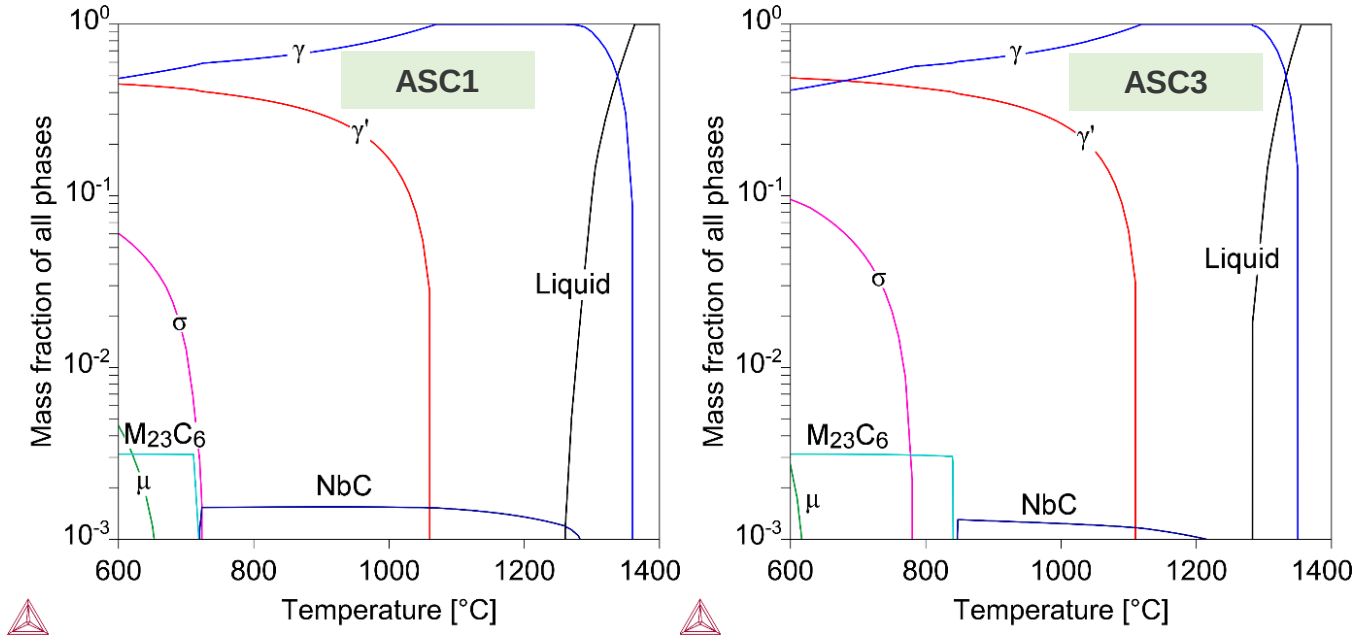

Thermo-Calc predictions for ASC1 and ASC3 using the TTNi8 database.

wt.%	Ni	Cr	Co	Fe	Al	Mo	W	Ti	Nb	C	B
ASC1	Bal.	10 - 20	15 - 20	2 - 8	2 - 8	2 - 5	2 - 5	0.0	4.0	0.016	0.006
ASC2	Bal.	10 - 20	15 - 20	2 - 8	2 - 8	2 - 5	2 - 5	1.0	3.0	0.016	0.006
ASC3	Bal.	10 - 20	15 - 20	2 - 8	2 - 8	2 - 5	2 - 5	2.0	2.0	0.016	0.006

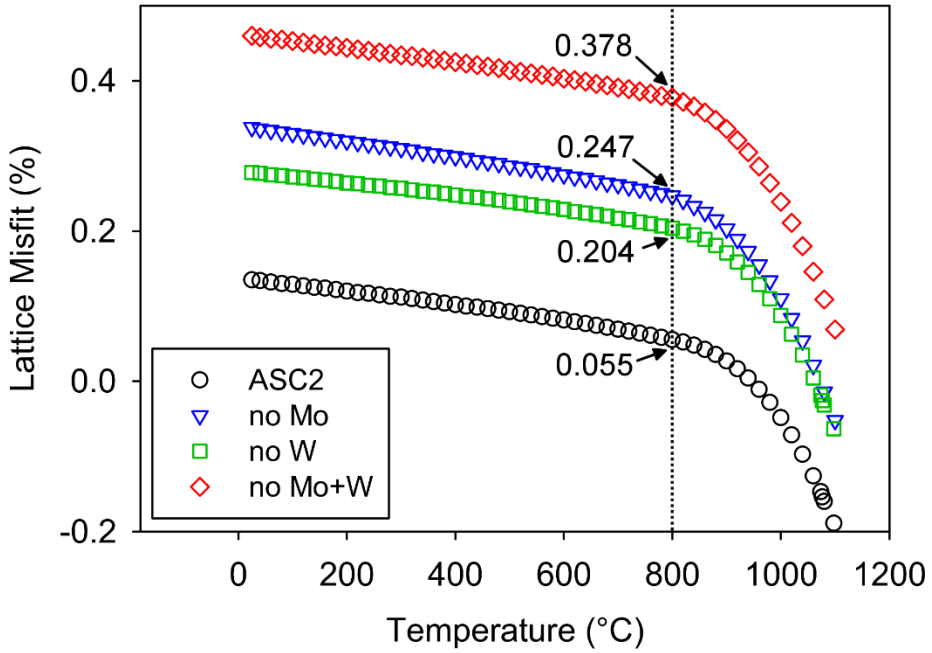

Lattice misfit calculated using JMatPro for the ASC2 composition and with or without Mo and/or W, after aging at 800°C for 16h.

Procedure

Melting and Fabrication

- High-purity, industrial grade, stock material + Ni30Cr30Co master alloy made using steps of VIM+ESR to reduce the oxygen concentration from Cr
- Vacuum induction melting ~7 kg ingots
- Chemistry analysis on a 2 mm slice cut from the ingots
- XRF and LECO analysis
- Homogenization following a computationally optimized heat treatment schedule (+/-1% inhomogeneity throughout the ingot)
- Conditioning of the ingots
- Fabrication using steps of forging followed by hot rolling
- Aging
- Testing using ASTM standards (E-8 for tension)

Characterization

Microstructure

- Nano-sized γ' precipitates (below 80 nm at 800°C)
- Fraction between 25 and 36% with the increase related to aging time and temperature.
- Significant coarsening observed at 900°C after 160h

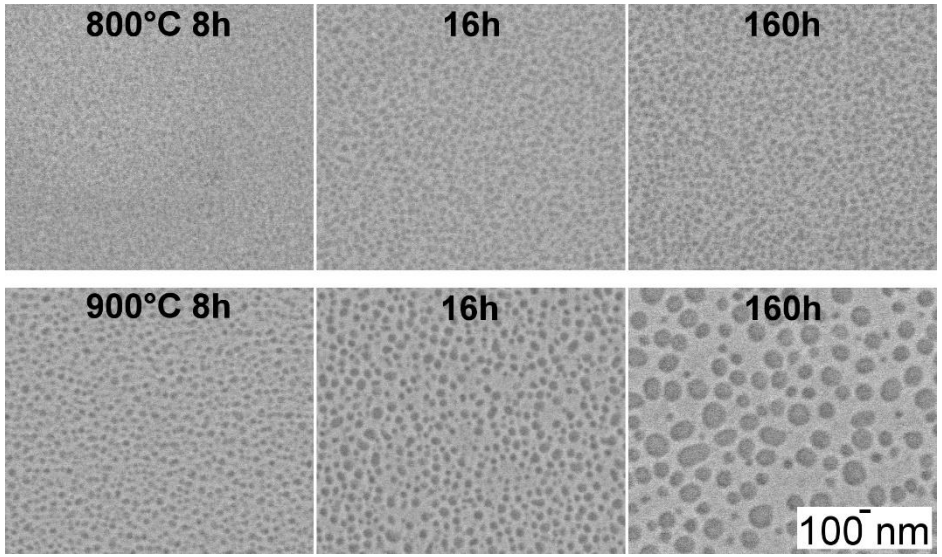

◄ γ' in ASC2 following aging at 800 or 900°C for 8, 16, or 160h.

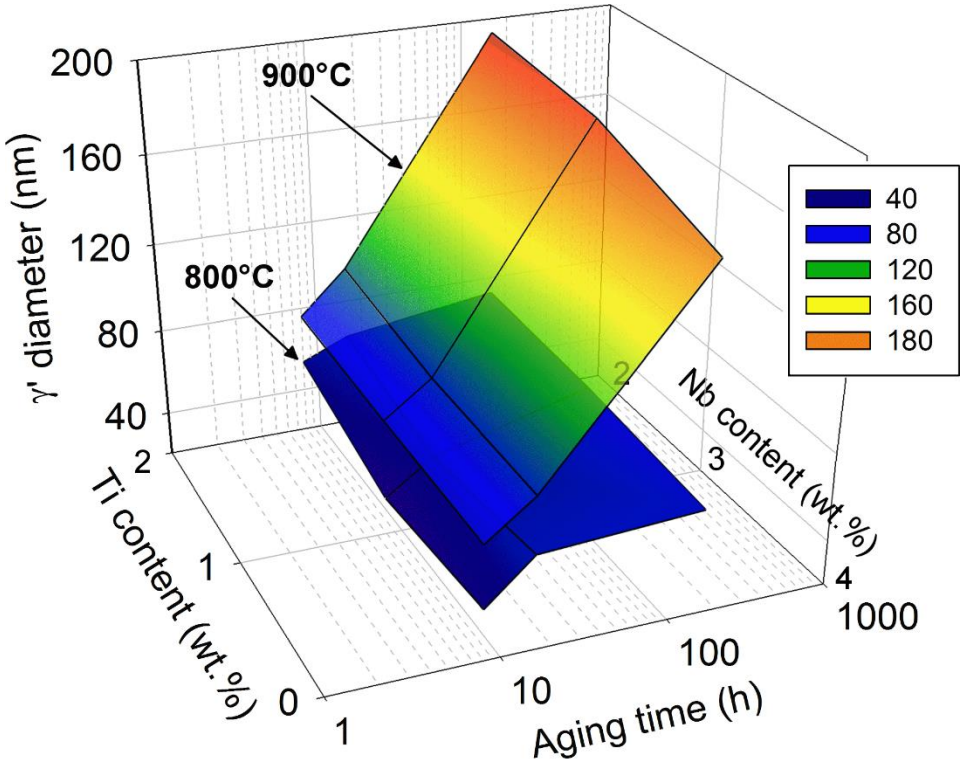

γ' size in the ASC alloys following aging at 800 or 900°C for 8, 16, or 160h plotted as a function of the Ti and Nb contents.

Characterization

Microstructure

- Equiaxed grain structure of ASTM 2 (~170 µm)
- Primary MC carbides (Ti-containing NbC) of 1.8 µm average size
- $M_{23}C_6$ carbides along the grain boundaries following aging at 800°C of width from 50 to 160 nm after 16h and 160h aging
- Elongated Ti-lean NbC carbides along the grain boundaries following aging at 900°C

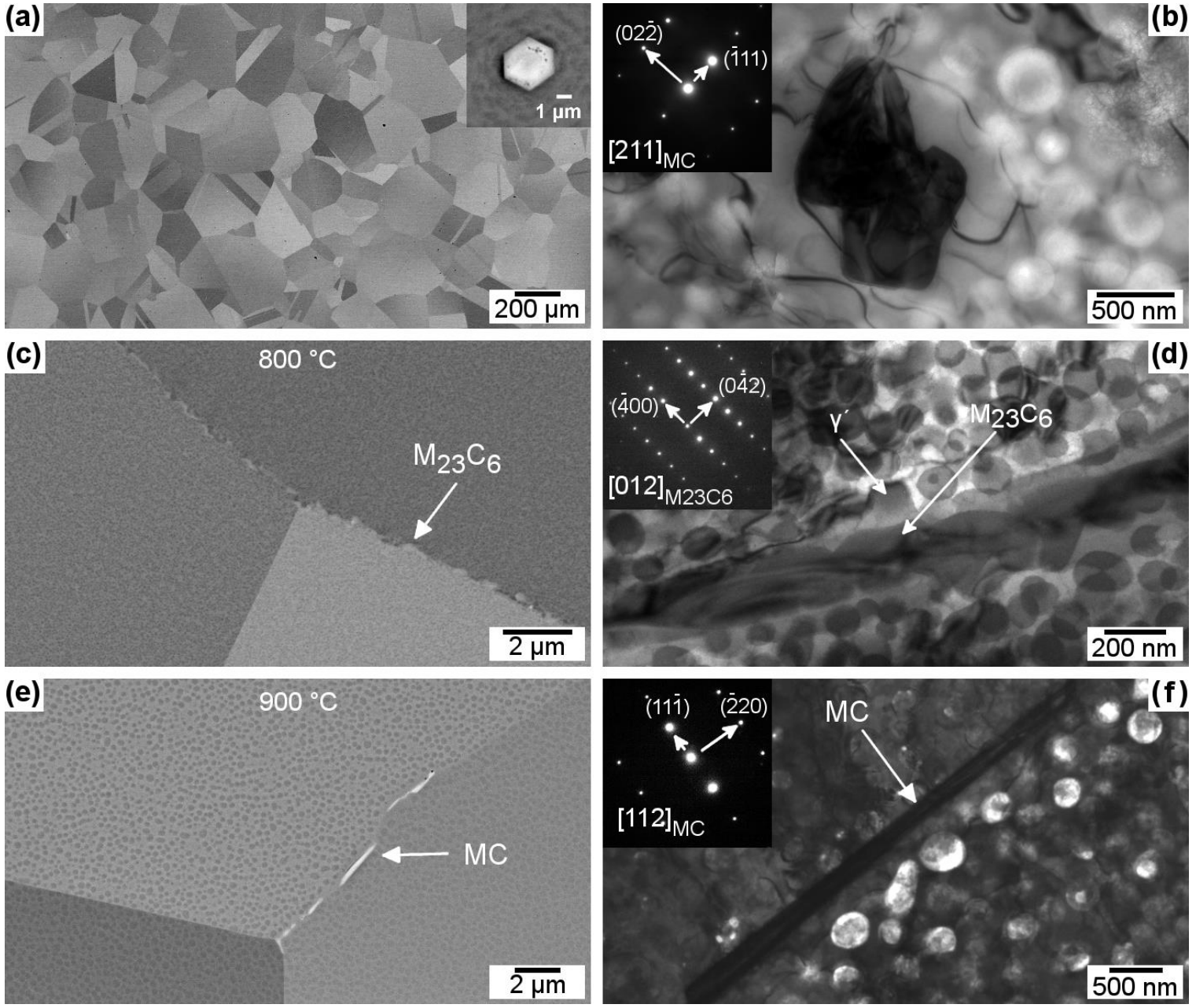

Mechanical Properties

Tensile Testing

- 1318 MPa ultimate tensile strength on average at room temperature. Decreased to ~1070 MPa at 700°C and 850 MPa at 800°C
- 0.2% yield stress of 932 MPa on average at room temperature, 905 MPa at 700°C and 774 MPa at 800°C
- Elongation of 18% at room temperature. Falls ~5% at 700°C and 1.7% at 800°C

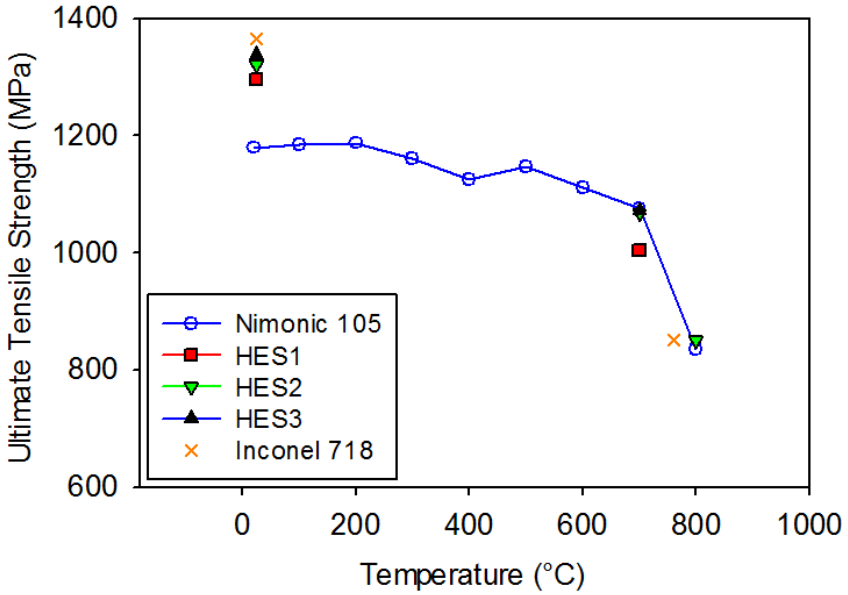

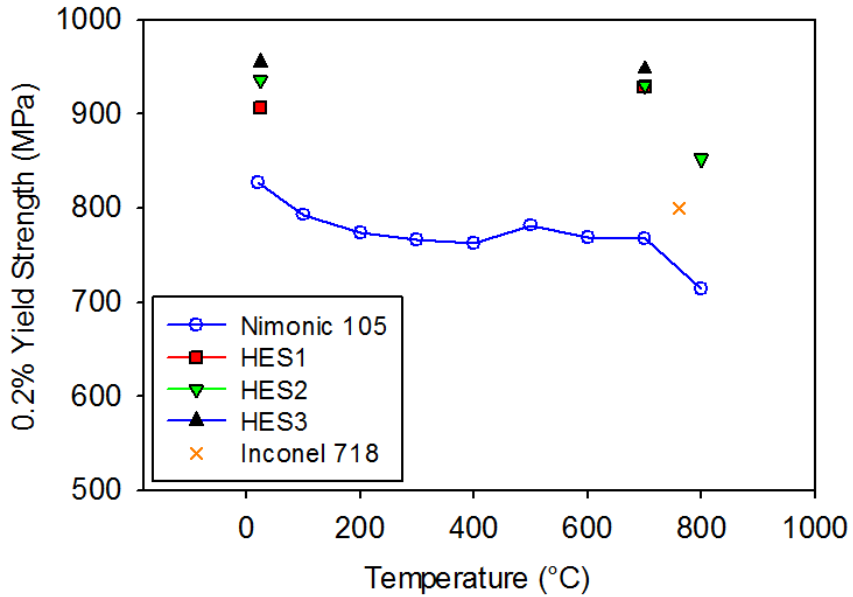

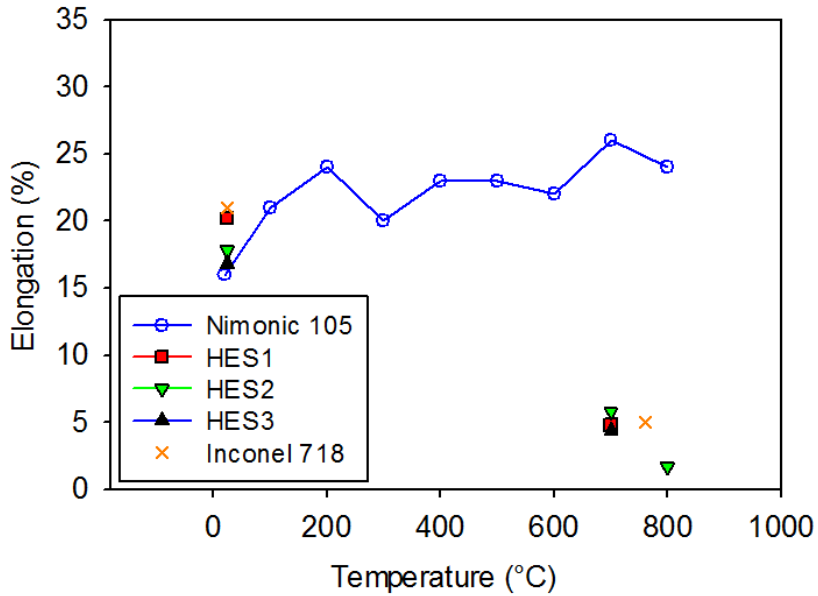

Mechanical Properties

Fracture Surfaces

Nominally similar after testing at 700 or 800°C

(a) Primarily intergranular failure with distinct grain facets

(b) Mixed intergranular and transgranular failure

(c) Transgranular failure

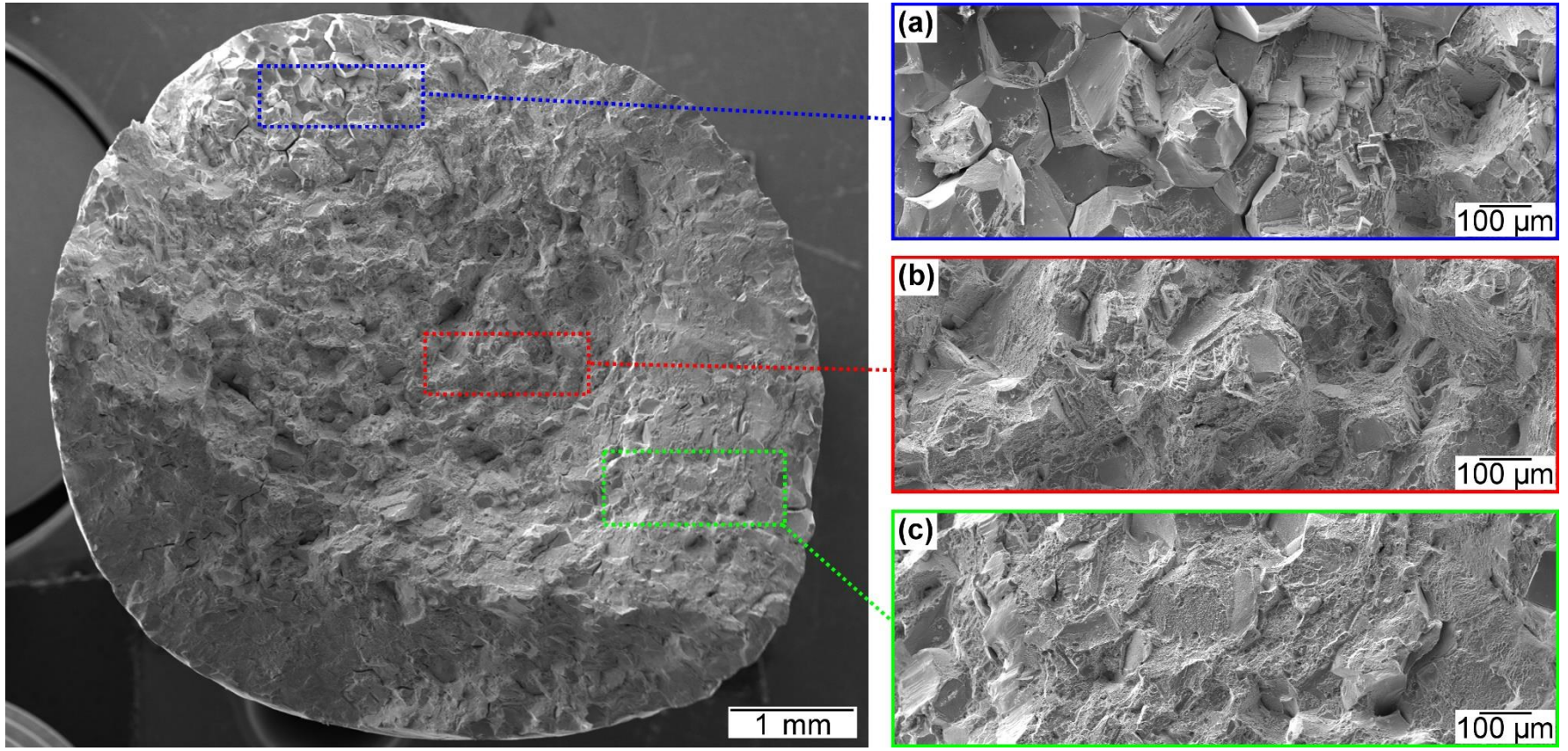

► **Fracture surface of ASC2 after testing at 700°C.**

Deformation Behavior

Gleeble Testing

- Testing performed to a final strain of 0.5, for temperatures of 1050, 1090, 1130, 1170 and 1210°C and strain rates of 0.001, 0.01 and 0.1/s
- Cylinders measuring 8.2 mm in diameter and 12.2 mm in height were cut from the wrought processed plates
- Starting grain size was ASTM 2 (~ 170 µm)

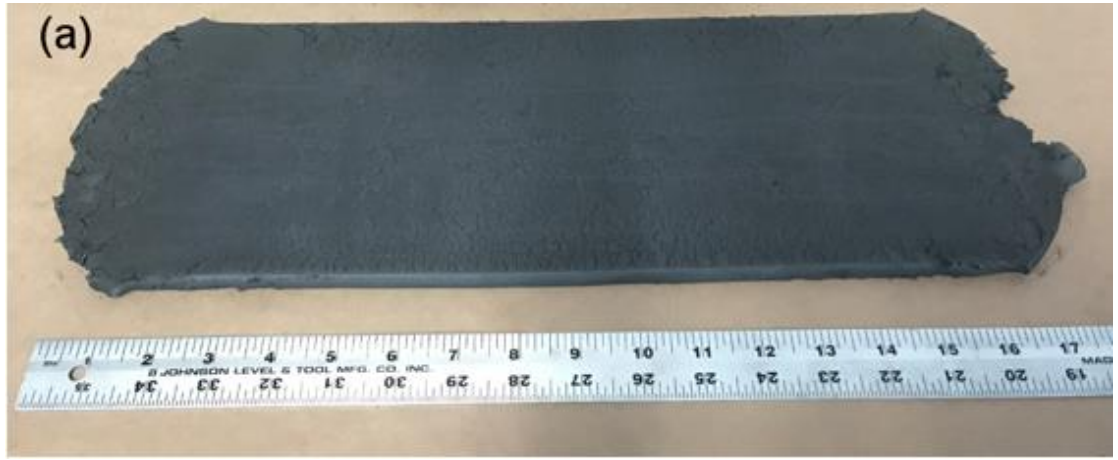

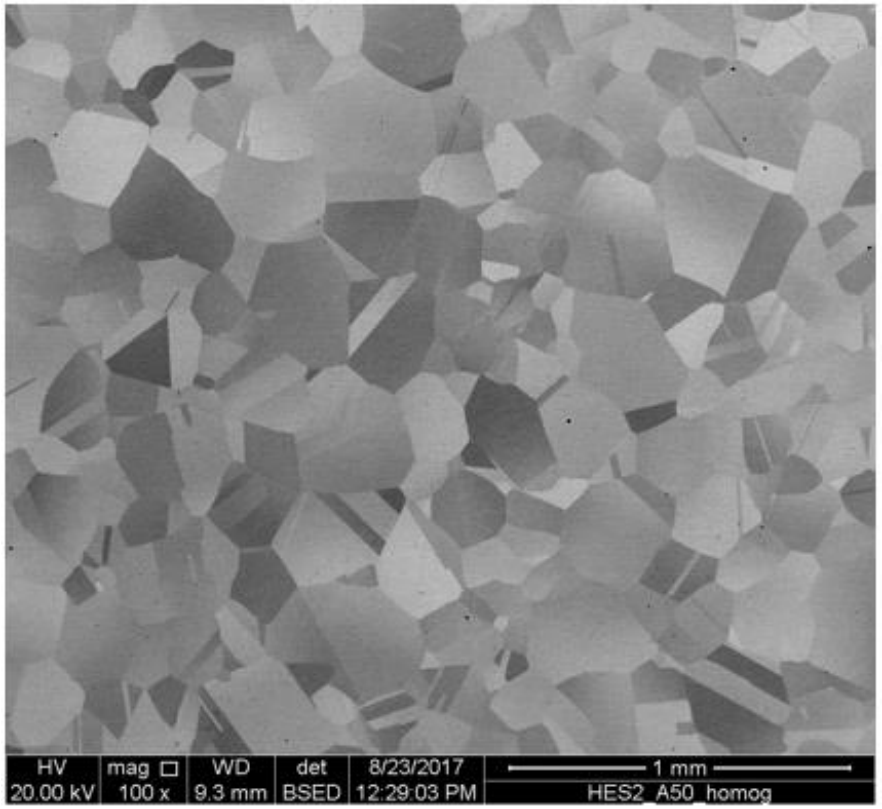

Deformation Behavior

Gleeble Testing

- Stress-strain curves from Gleeble testing
- Most curves show evidence of strain hardening followed by softening indicative of DDRX and decreasing with deformation temperature from the restricted dislocation mobility
- Decrease in peak strain with decreasing deformation temperature
- Near steady state at high temperature and low strain rates indicative of near-superplastic deformation

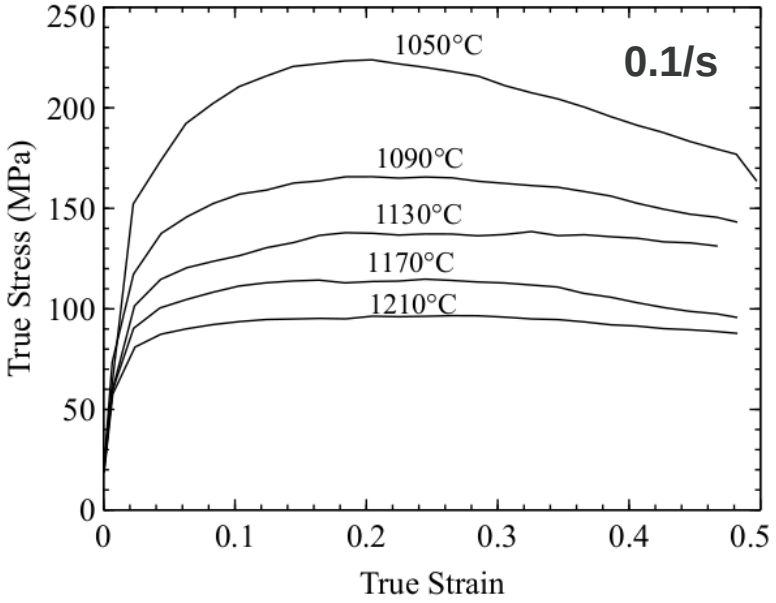

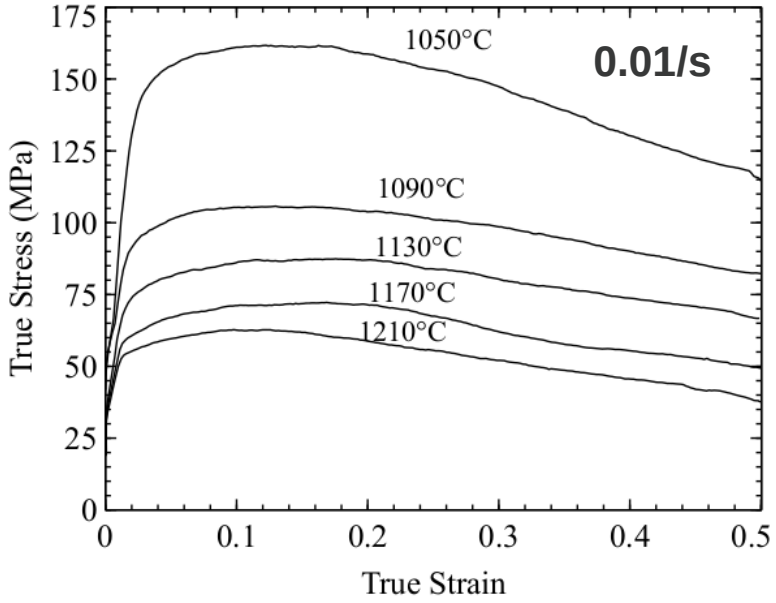

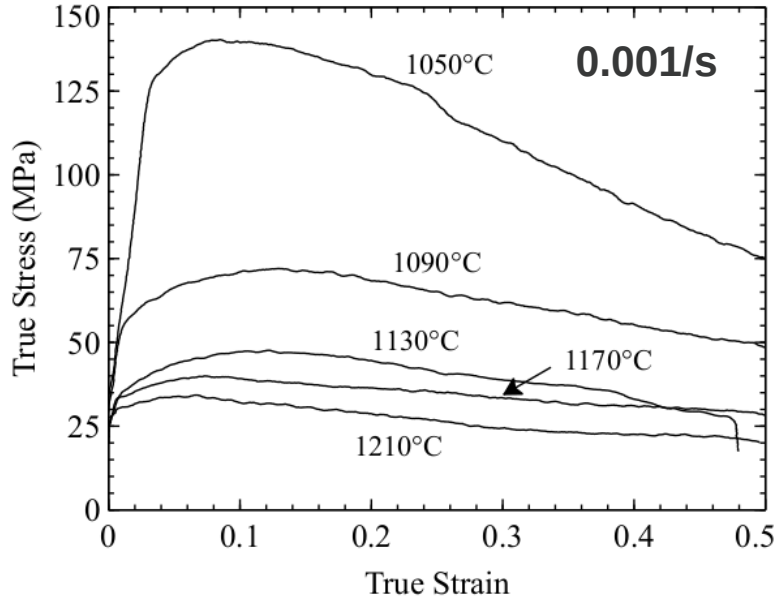

Deformation Behavior

EBSD

IPF maps with high angle grain boundaries.

Intragranular misorientation maps (or geometrically necessary dislocation maps, with high angle boundaries in black.

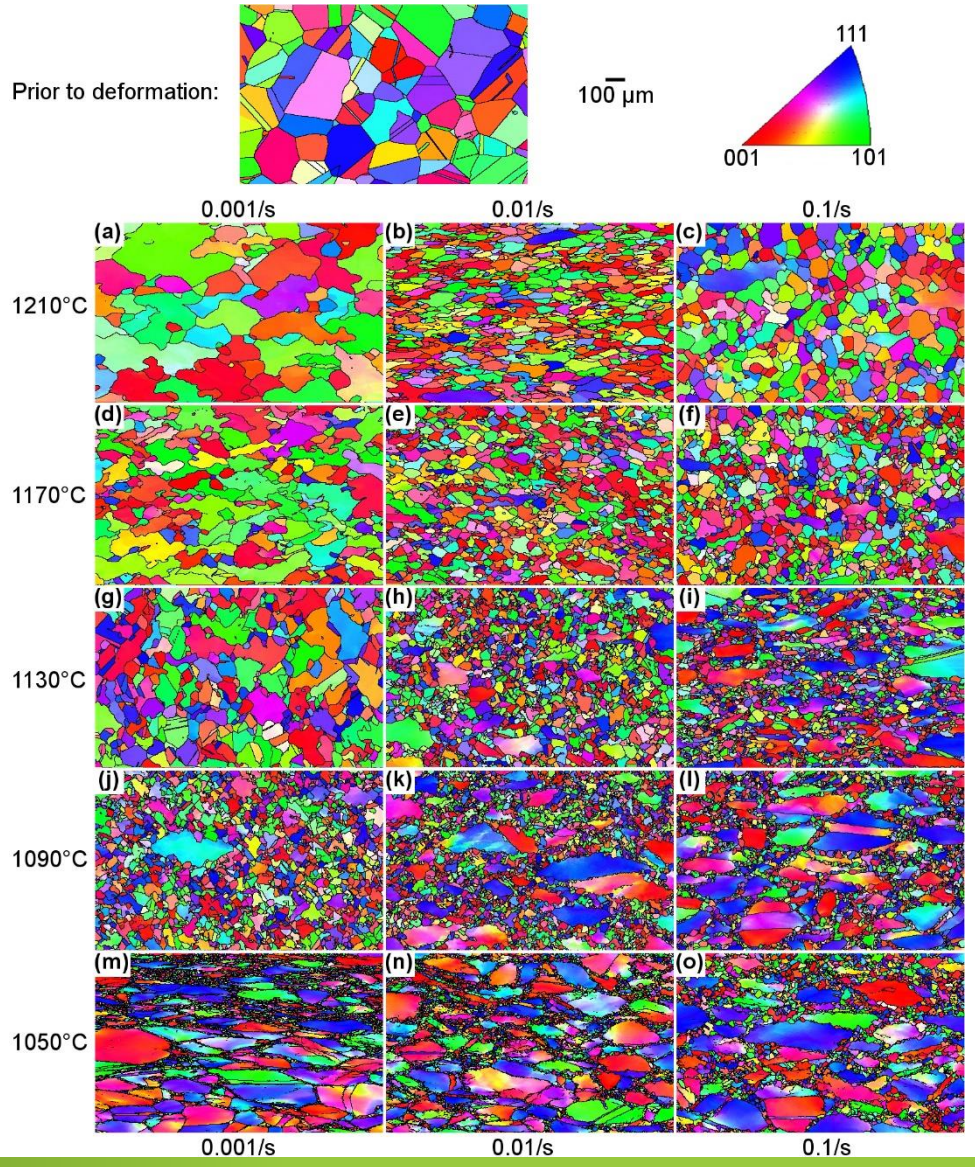

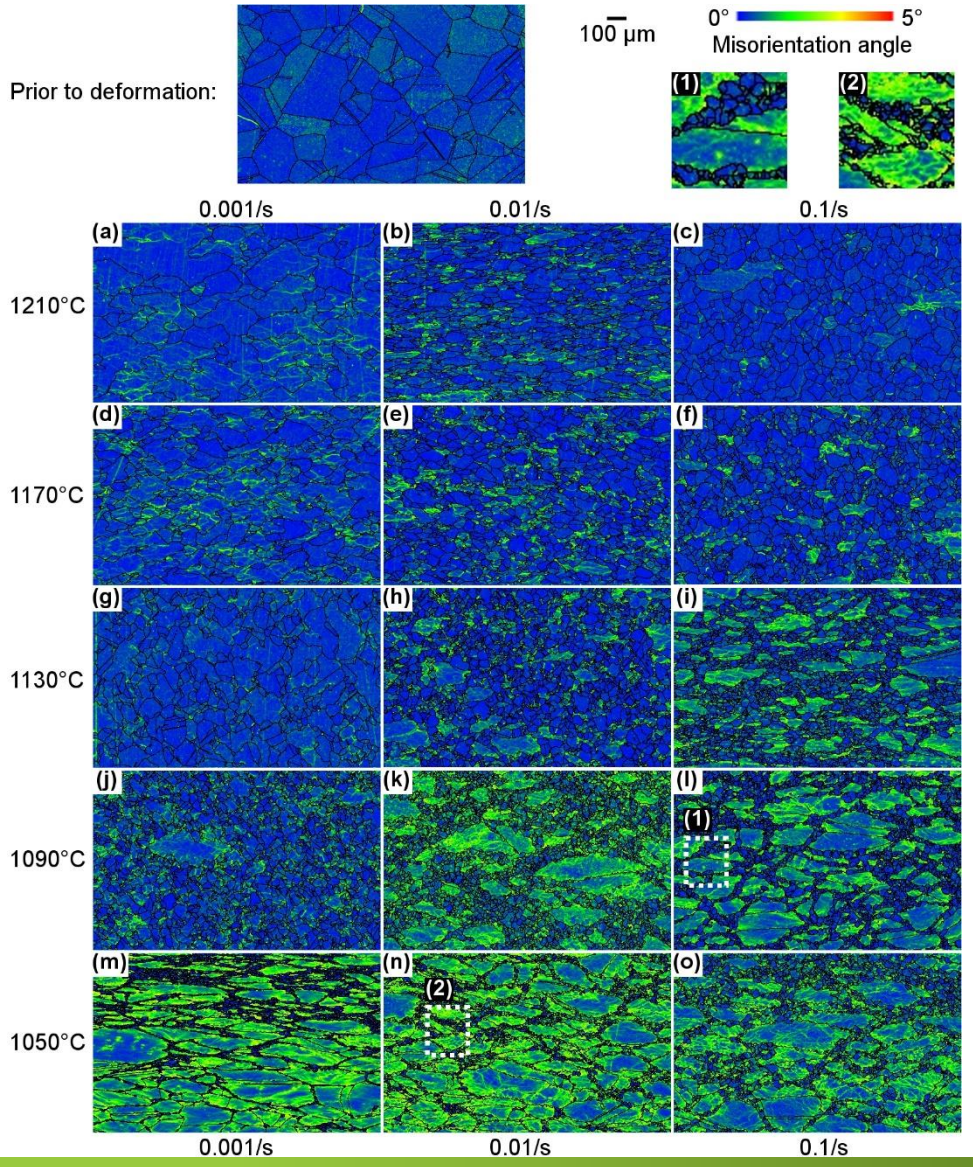

Deformation Behavior

EBSD

IPF maps with high angle grain boundaries.

Intragranular misorientation maps (or geometrically necessary dislocation maps, with high angle boundaries in black.

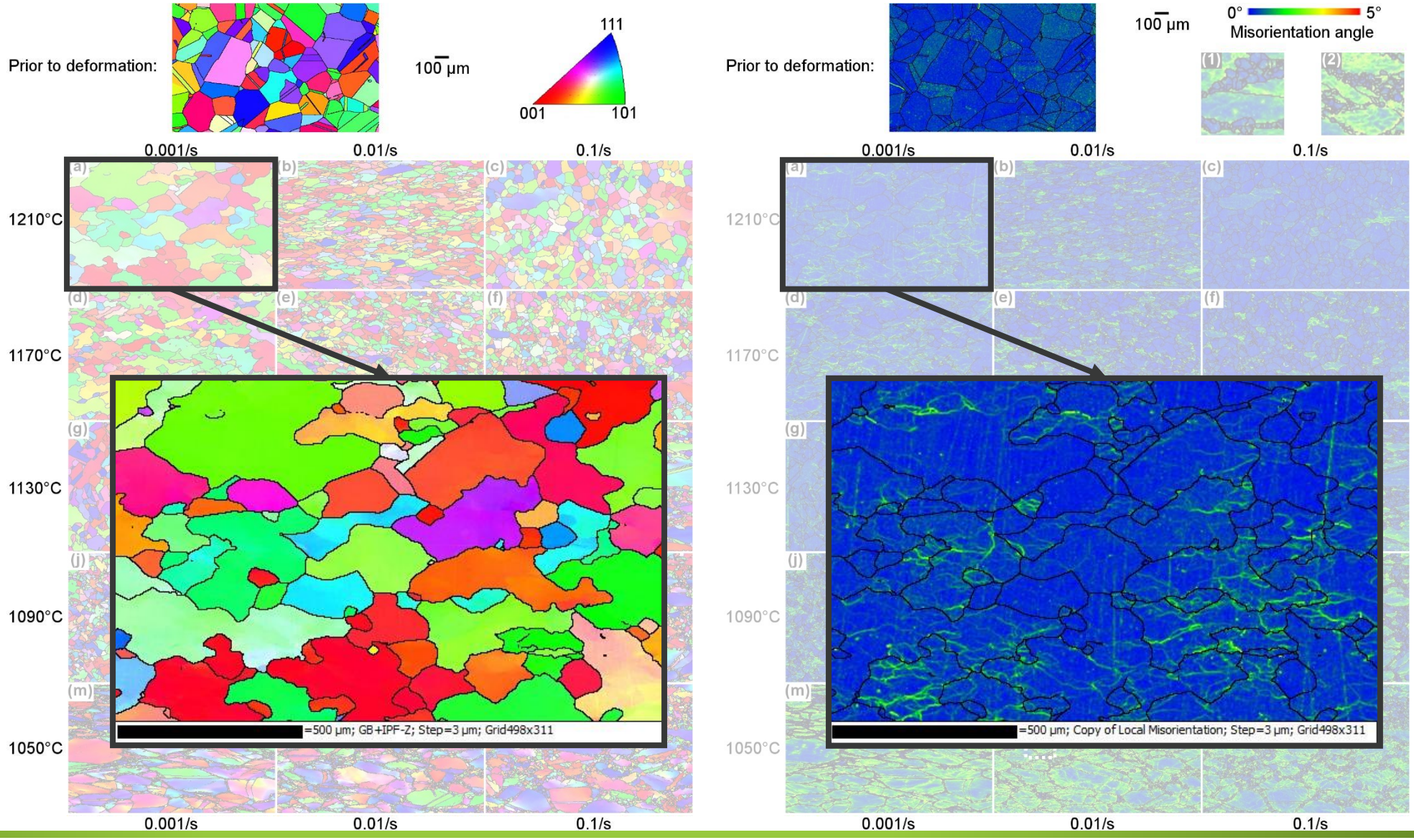

Deformation Behavior

EBSD

IPF maps with high angle grain boundaries.

Intragranular misorientation maps (or geometrically necessary dislocation maps, with high angle boundaries in black.

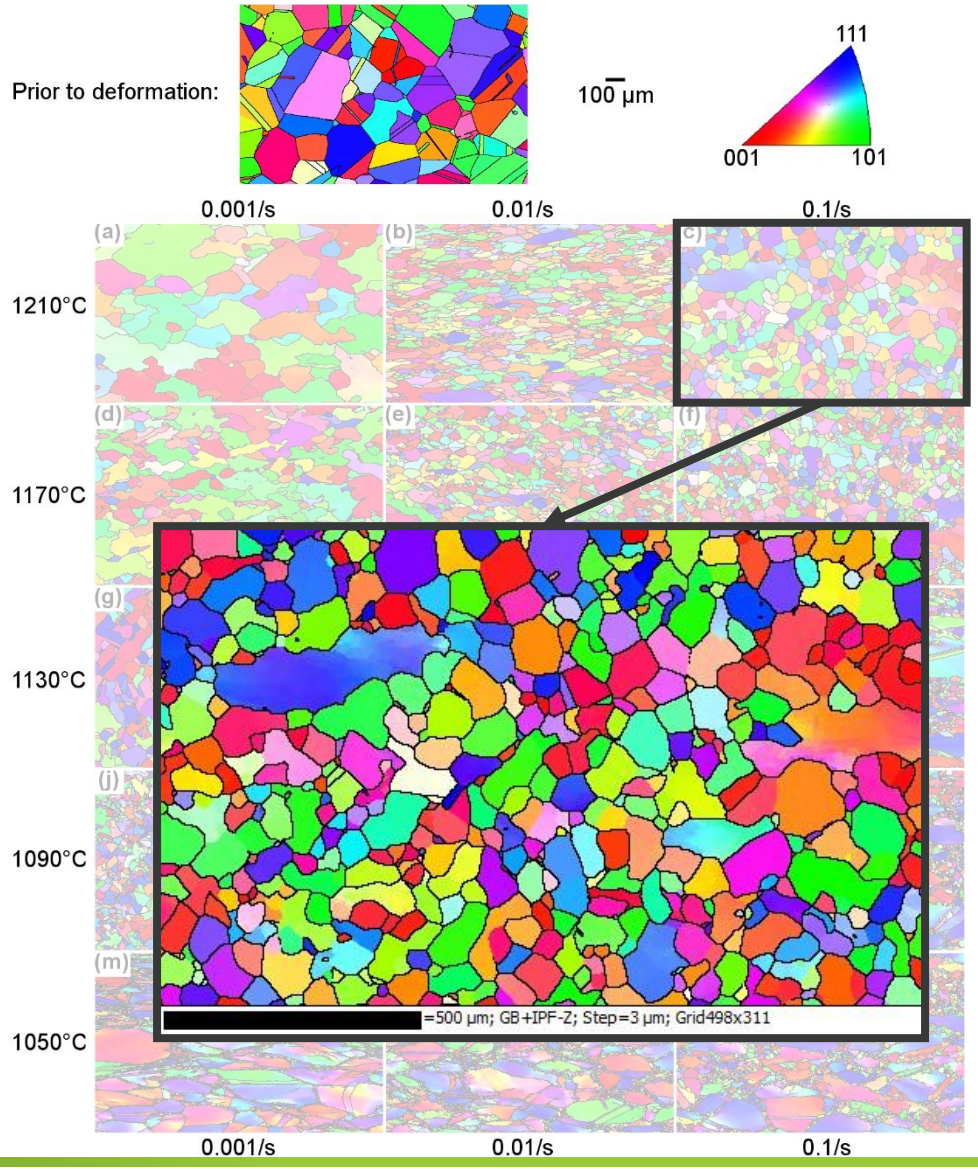

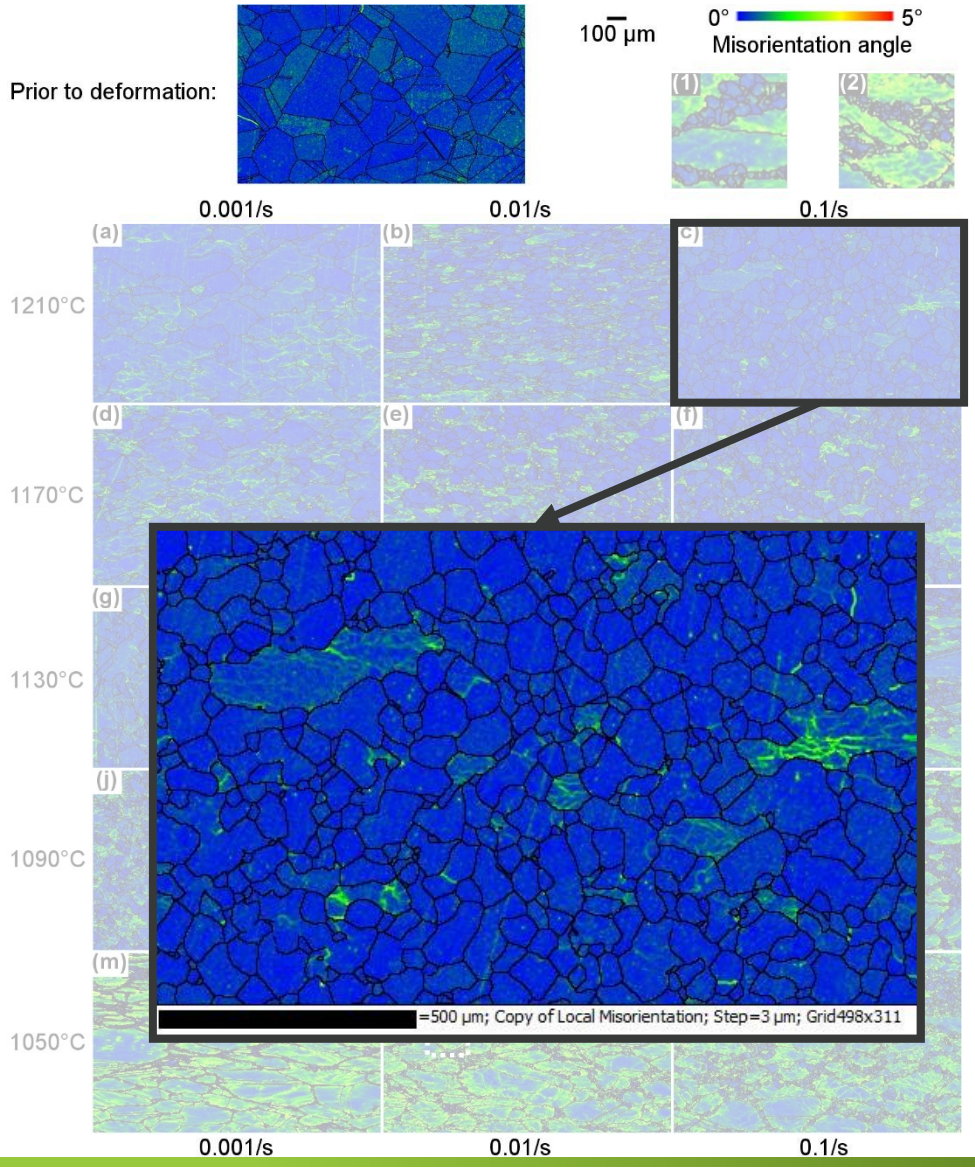

Deformation Behavior

EBSD

IPF maps with high angle grain boundaries.

Intragranular misorientation maps (or geometrically necessary dislocation maps, with high angle boundaries in black.

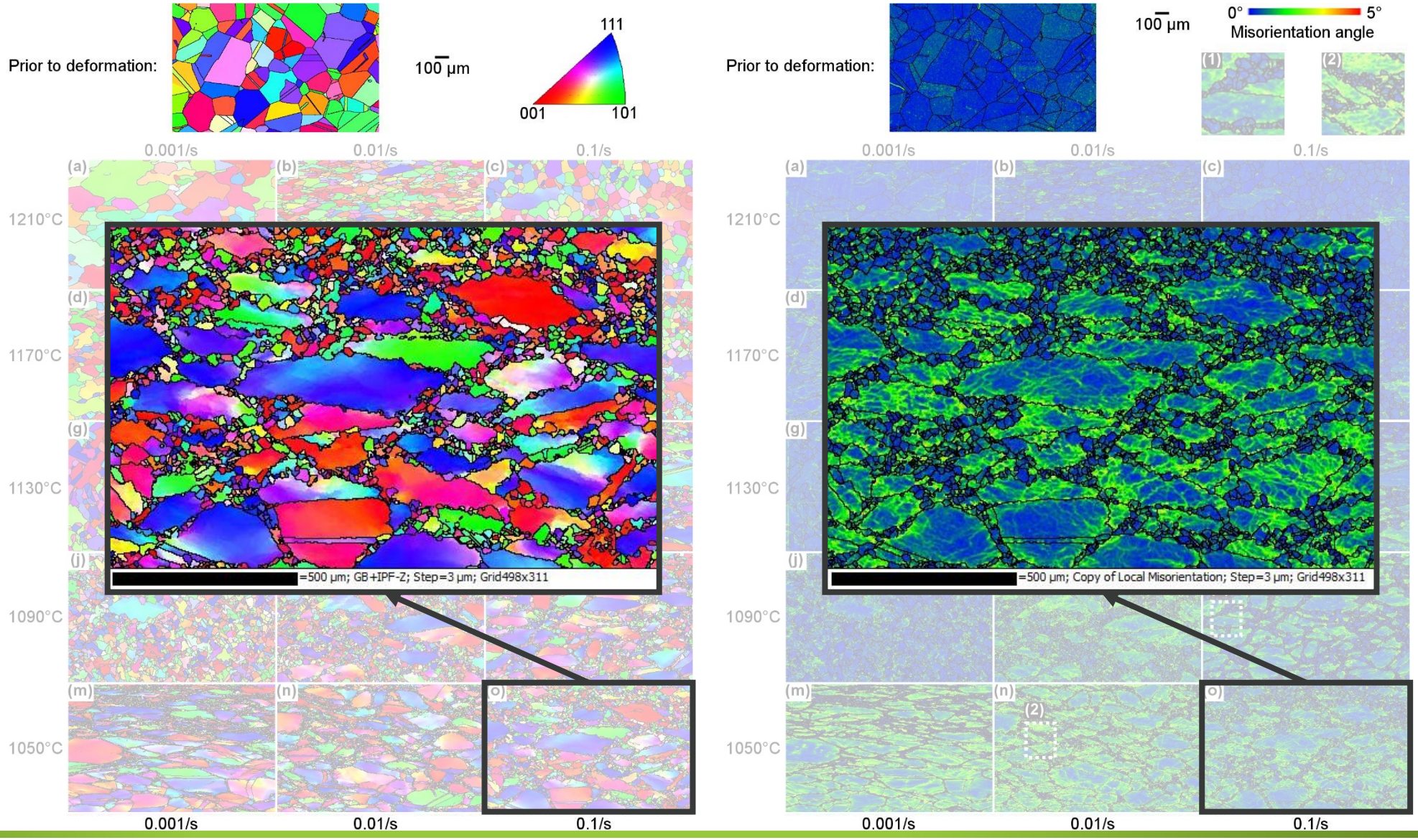

Deformation Behavior

Flow Stress Modeling

- Obtain model equations and parameters for hot deformation of the alloys
- Using the Zener-Hollomon parameter (Z)

$$Z = \dot{\varepsilon}\exp\left(\frac{Q}{RT}\right)$$

$$\dot{\varepsilon} = AF(\sigma)\exp\left(-\frac{Q}{RT}\right)$$

$$F(\sigma) = \begin{cases} \sigma^{n_1} & \alpha\sigma < 0.8 \\ \exp(\beta\sigma) & \alpha\sigma > 1.2 \\ \sinh(\alpha\sigma)^n & for\ all\ \sigma \end{cases}$$

$$\alpha = \frac{\beta}{n_1}$$

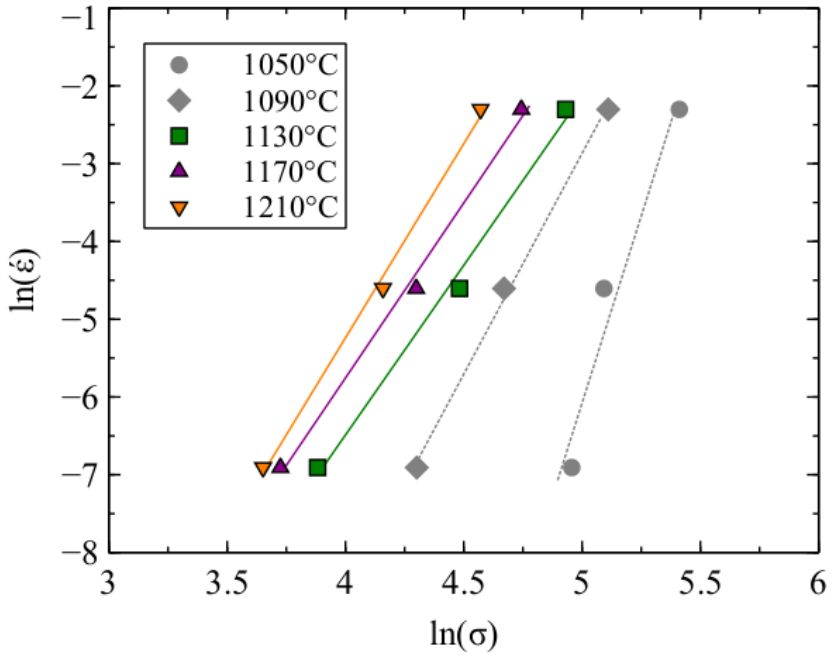

$n_1 = 4.62 \pm 0.33$

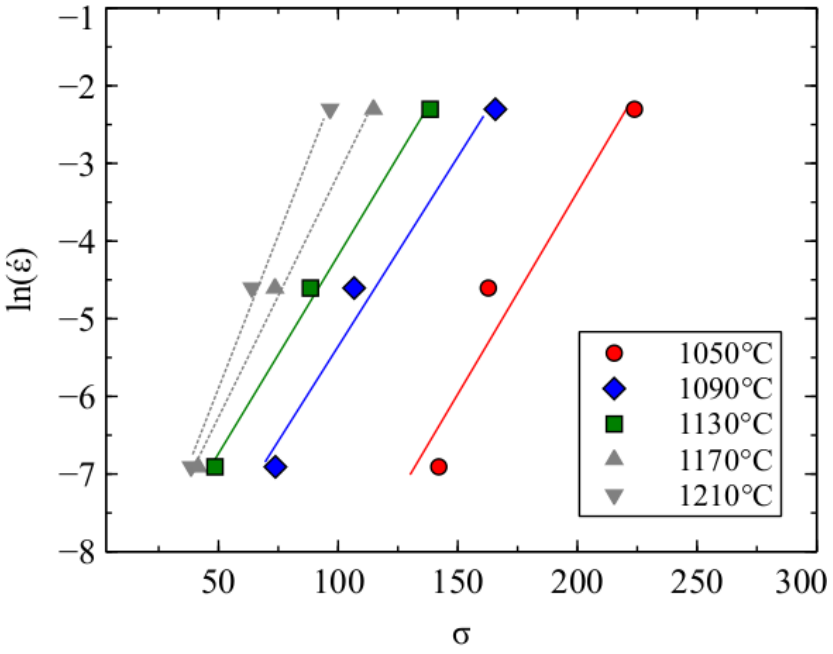

$\beta = 0.051 \pm 0.002$ MPa^{-1}

Deformation Behavior

Flow Stress Modeling

- Using two average slopes to calculate the activation energy
- Little correlation of the linear regression at 1050°C or 1000/T=0.76 K^{-1}

$$Q = R\left\{\frac{\partial \ln(\dot{\varepsilon})}{\partial \ln[\sinh(\alpha\sigma)]}\right\}_T \left\{\frac{\partial \ln[\sinh(\alpha\sigma)]}{\partial(1/T)}\right\}_{\dot{\varepsilon}}$$

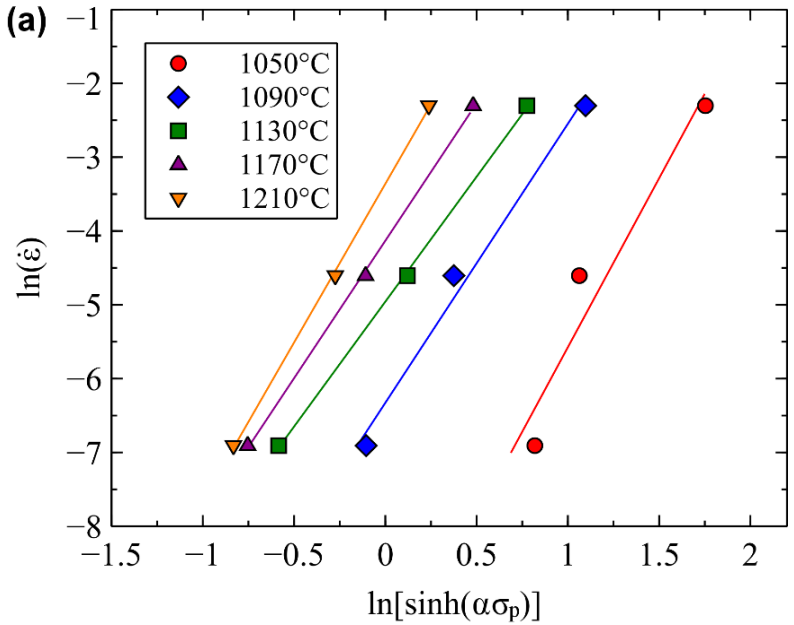

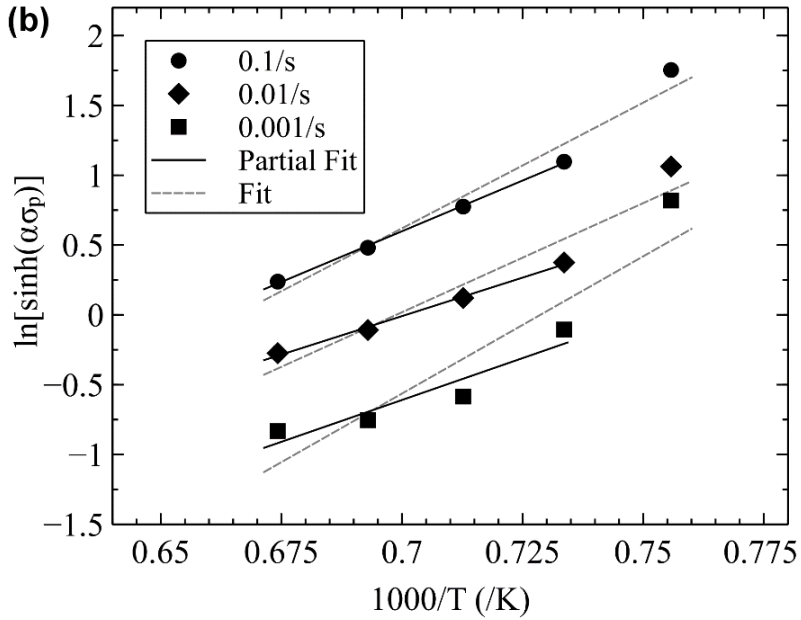

Average slope: 3.95 ± 0.48

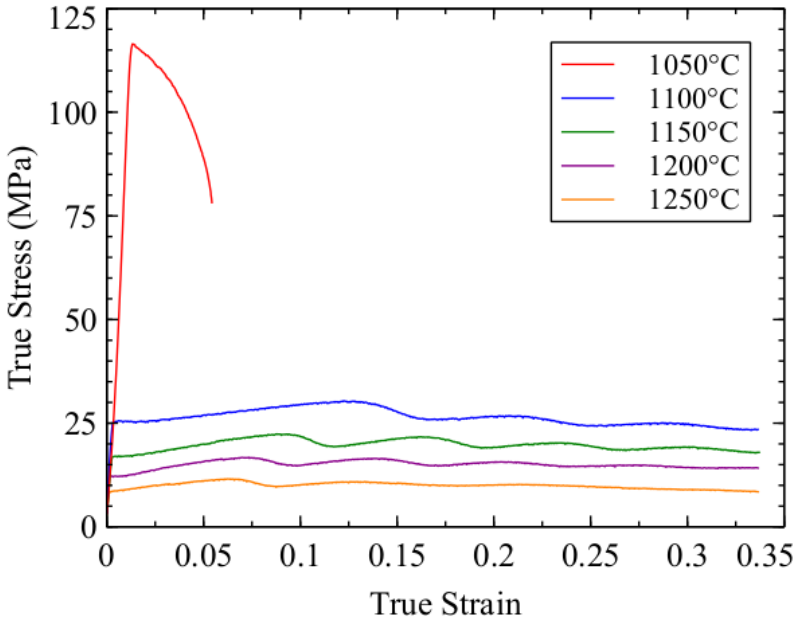

Hot tensile testing of HES3 (tests were stopped at 40% elongation)

Deformation Behavior

Flow Stress Modeling

- Plot ln(Z) vs ln(sinh(ασ)) to determine the constants of the Arrhenius equation
- Leads to the flow stress model for ASC2

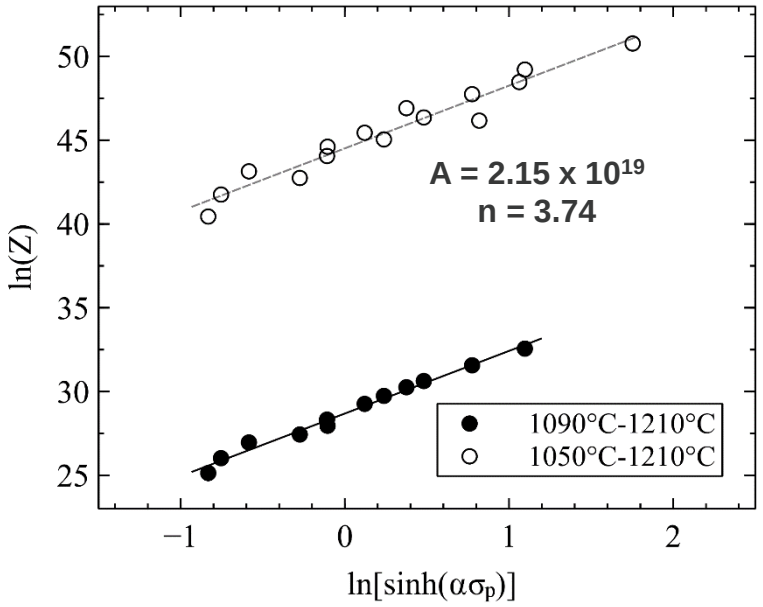

Flow stress model:

$$\dot{\varepsilon} = 2.15 \times 10^{19} \sinh\left(0.011\sigma_p\right)^{3.74} \exp\left(-\frac{583900}{RT}\right)$$

$\dot{\varepsilon}$ is the strain rate in s^{-1}, σp is the peak stress in MPa, R is the gas constant in $JK^{-1}mol^{-1}$ and T is the temperature in K

The predictions of the model were compared to the experimental data. The results were in good agreement at the exception of 1050°C – $0.001s^{-1}$ which shows that microstructural changes strongly affect the flow stress model.

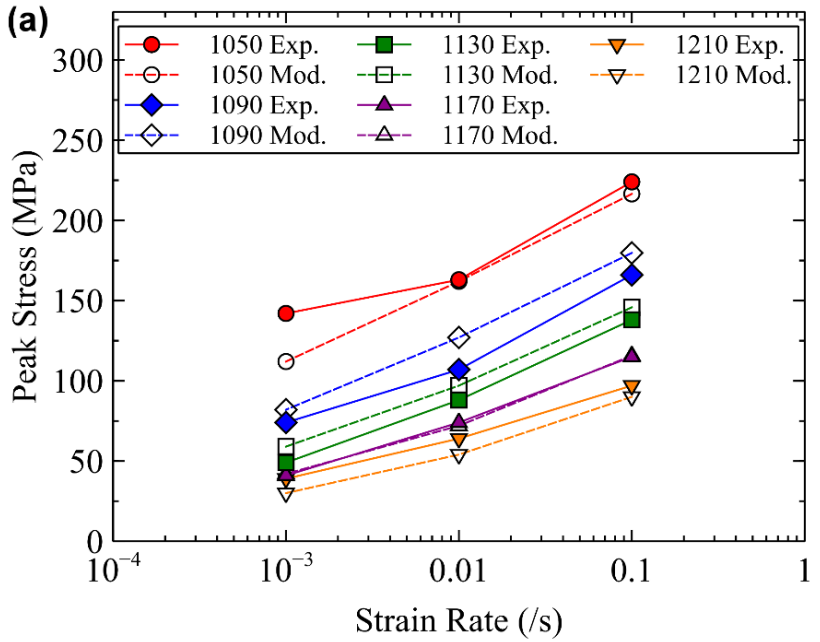

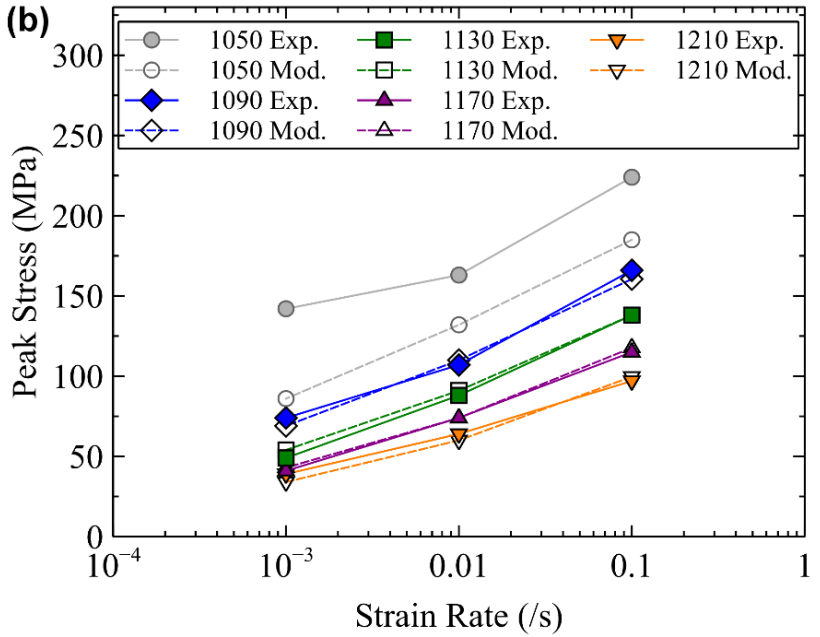

Deformation Behavior

Flow Stress Modeling

- Flow stress modeling can be used to obtain more information for each deformation mechanism
- Regroup processing parameters based upon strongest correlations of linear fit
- New calculations of activation energy, n and A parameters for each group

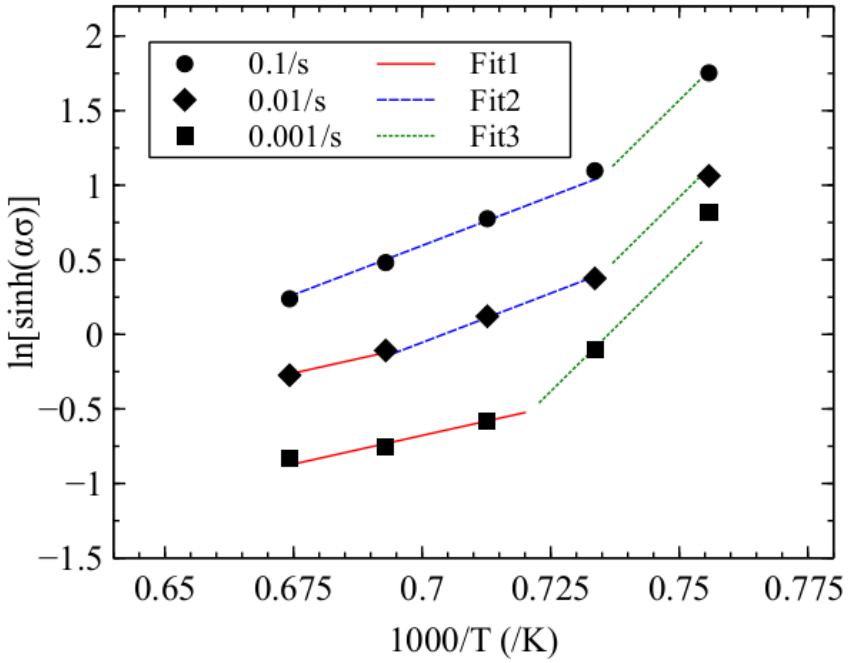

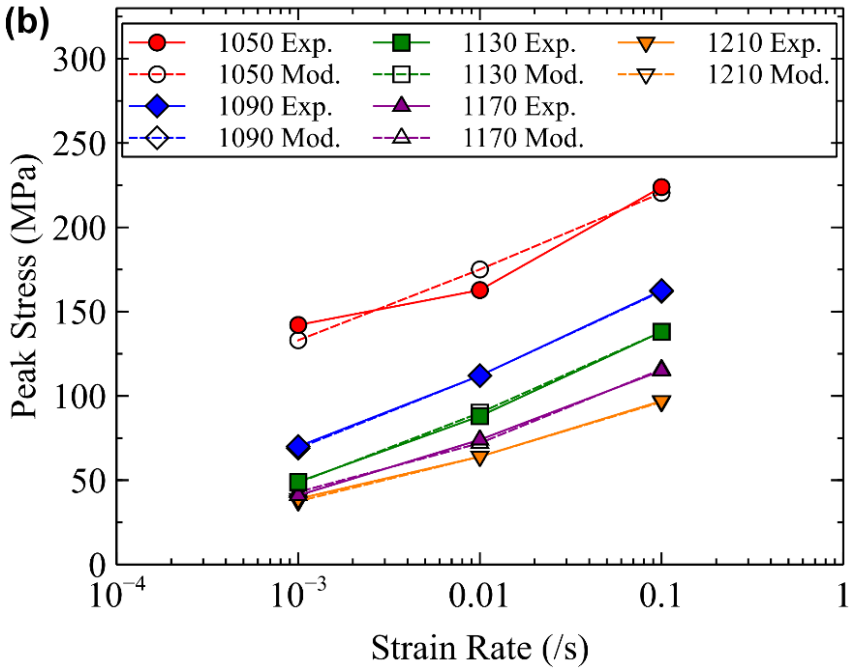

Q(Fit1) = 252 kJ/mol
Predominant near-superplastic

Q(Fit2) = 434 kJ/mol
Predominant recrystallization

Q(Fit3) = 1121 kJ/mol
Predominant dislocation-based plasticity

Deformation Behavior

Conclusion

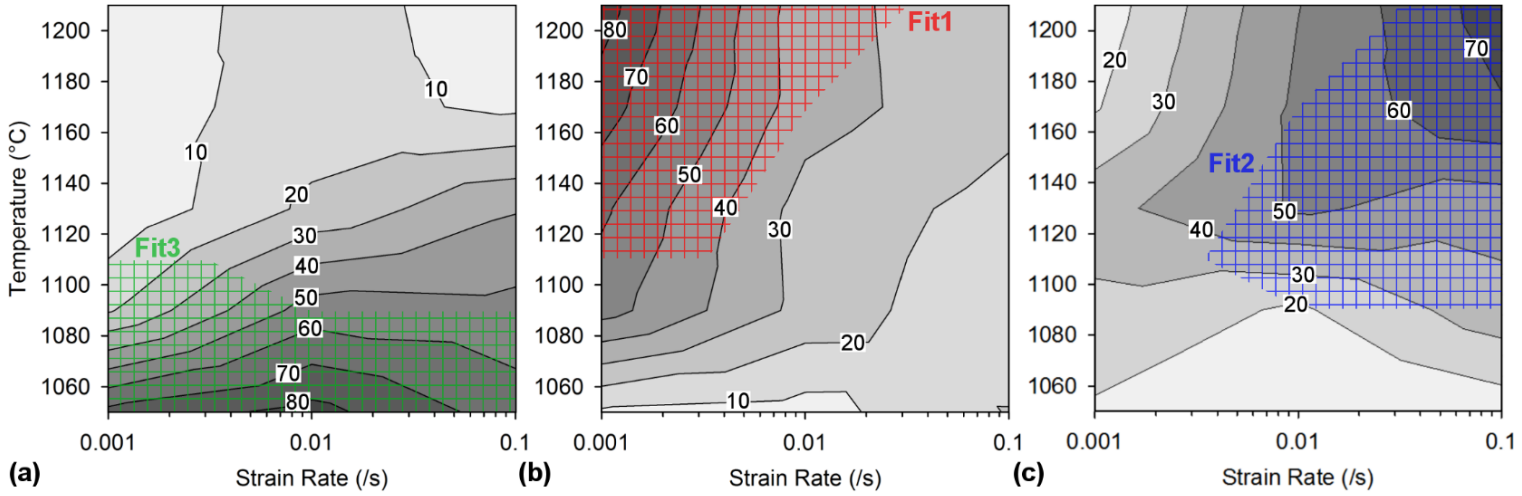

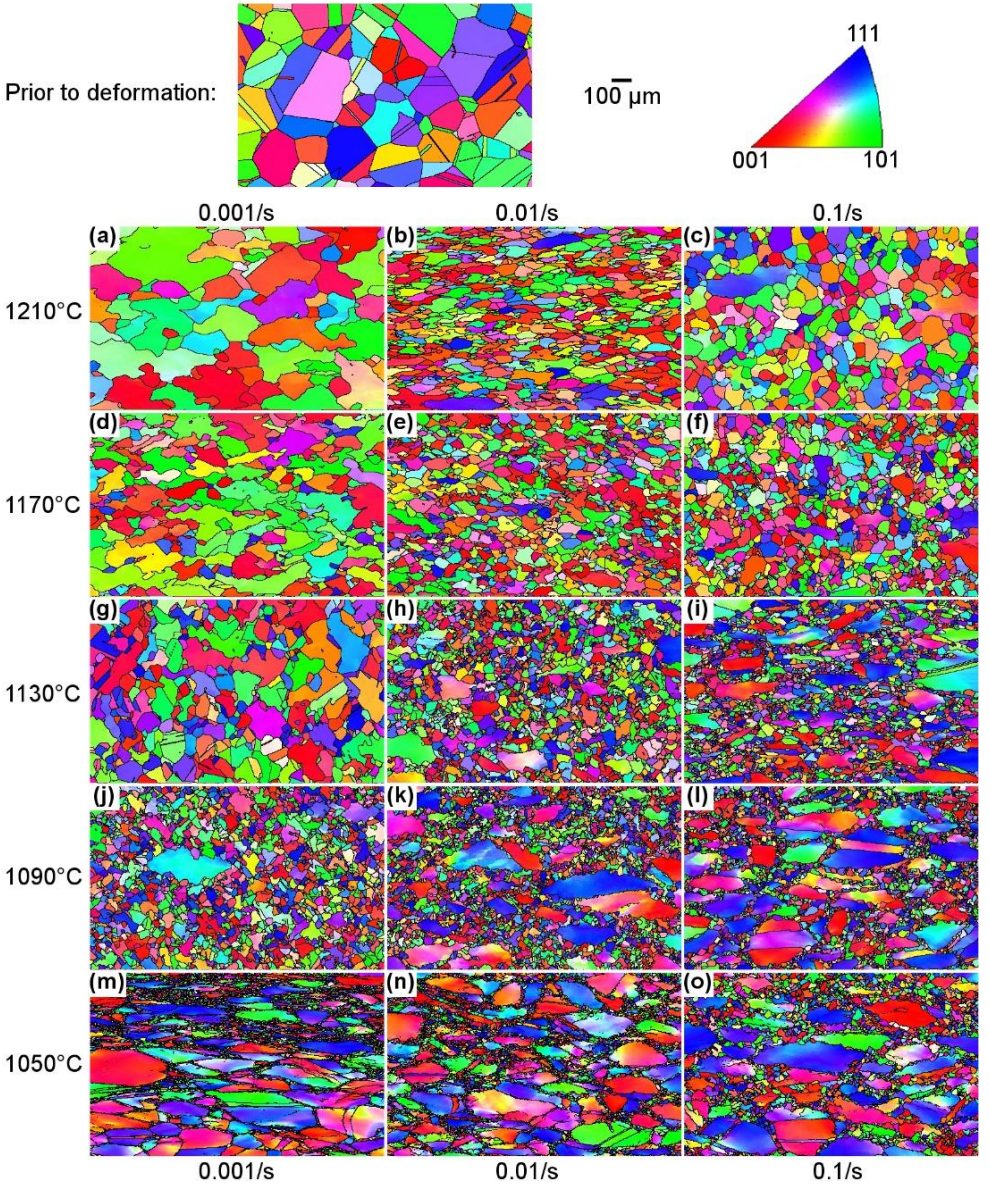

- Each group represent a predominant deformation behavior: near-superplastic for Fit1, recrystallization for Fit2 and dislocation-based for Fit3.
- Comparison with percent grains deformed **(a)**, recrystallized **(b)** and sub-structured (i.e. near-superplastic) **(c)** from EBSD.
- While not all conditions are in perfect agreement the general trends are in good agreement and the model provide the activation energy and materials constant for each deformation mechanism.

Undesirable phases

Melting and Forging

Alloys of identical compositions and stock material. Melted in same furnace and heat treated identically.

In Heat 2, higher temperatures of the melt pool, Al in liquid longer than in Heat 1. (3.5 minutes as compared to 1 minute.)

Eutectic constituent with NiAl phase remained after homogenization of Heat 2.

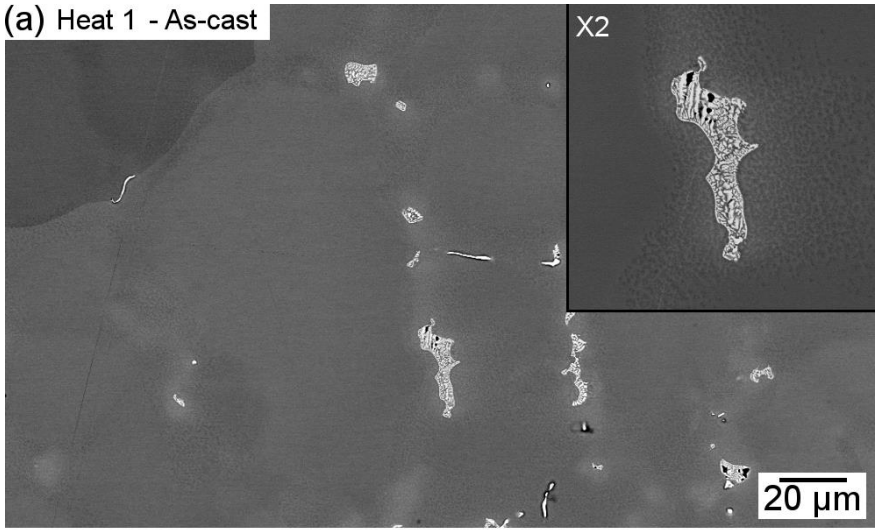

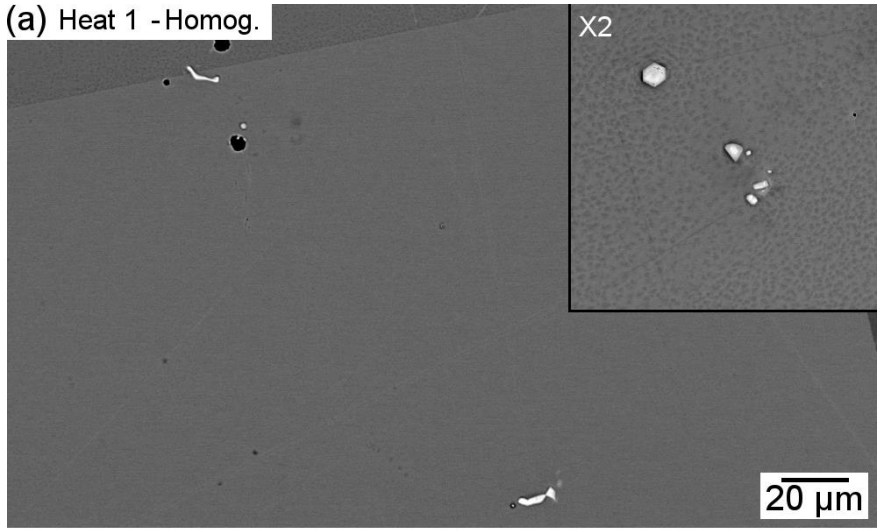

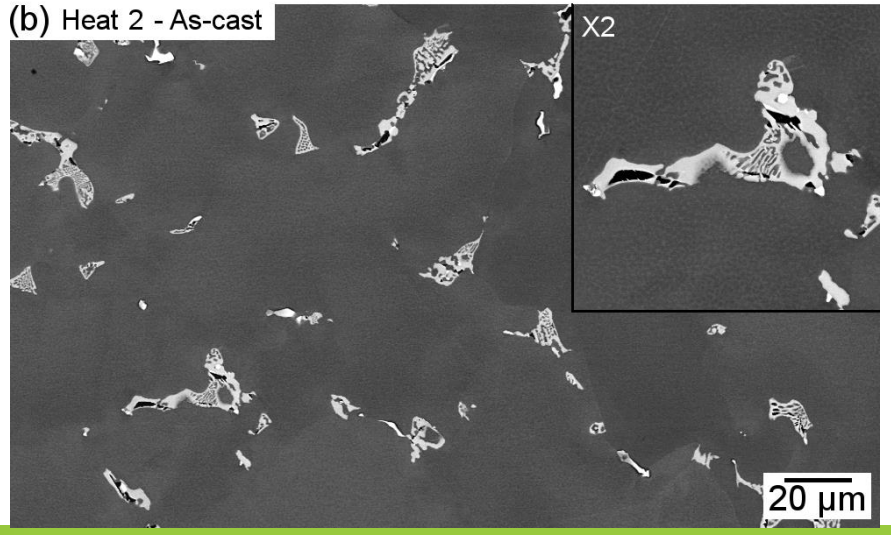

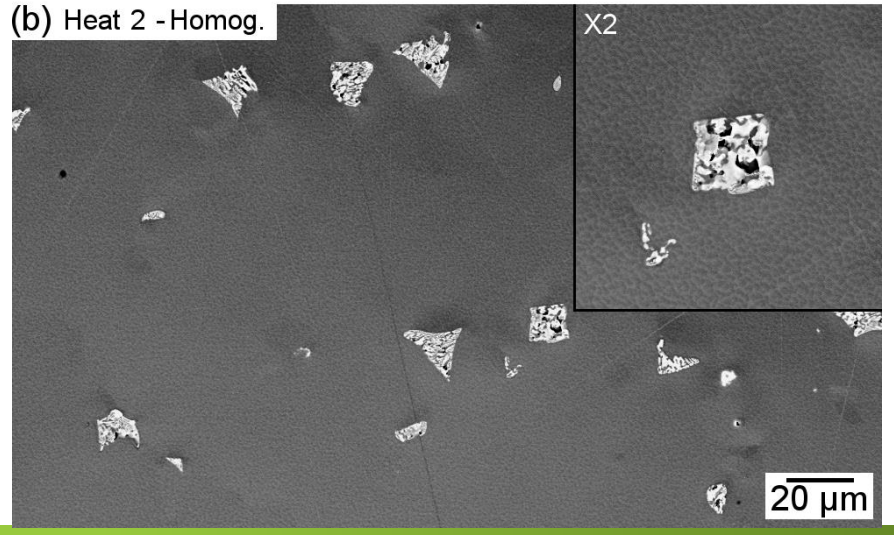

Undesirable phases

Melting and Forging

- From cast to homogenized: elongated to blocky with concave edges
- NiAl not predicted in the composition of the alloys from Thermo-Calc
- Superheat temperature for the alloy: 1380 + 50°C
- Melting temperature of NiAl: 1690°C

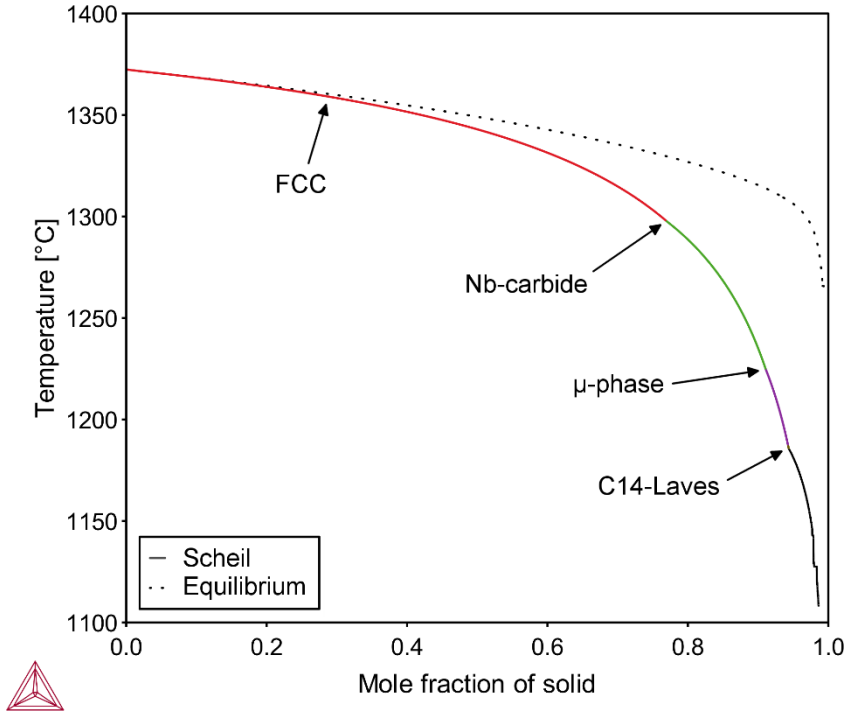

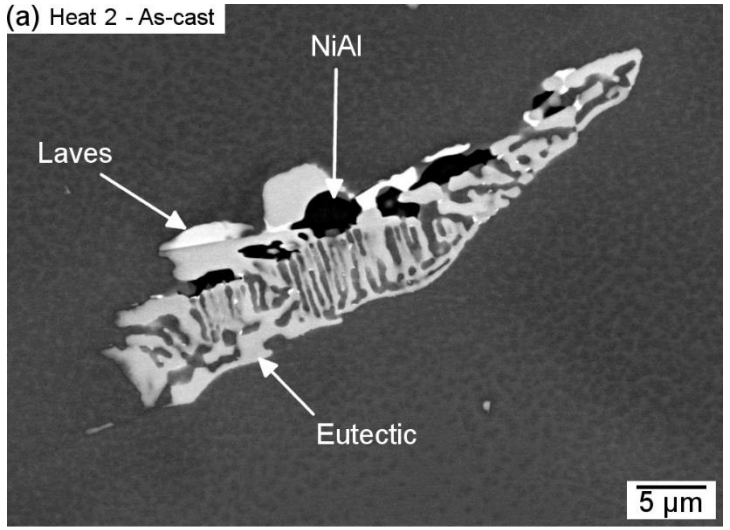

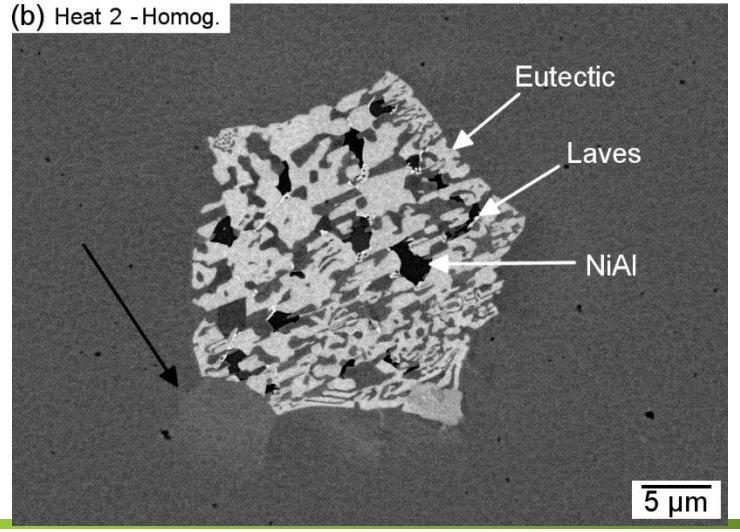

Undesirable phases

Melting and Forging

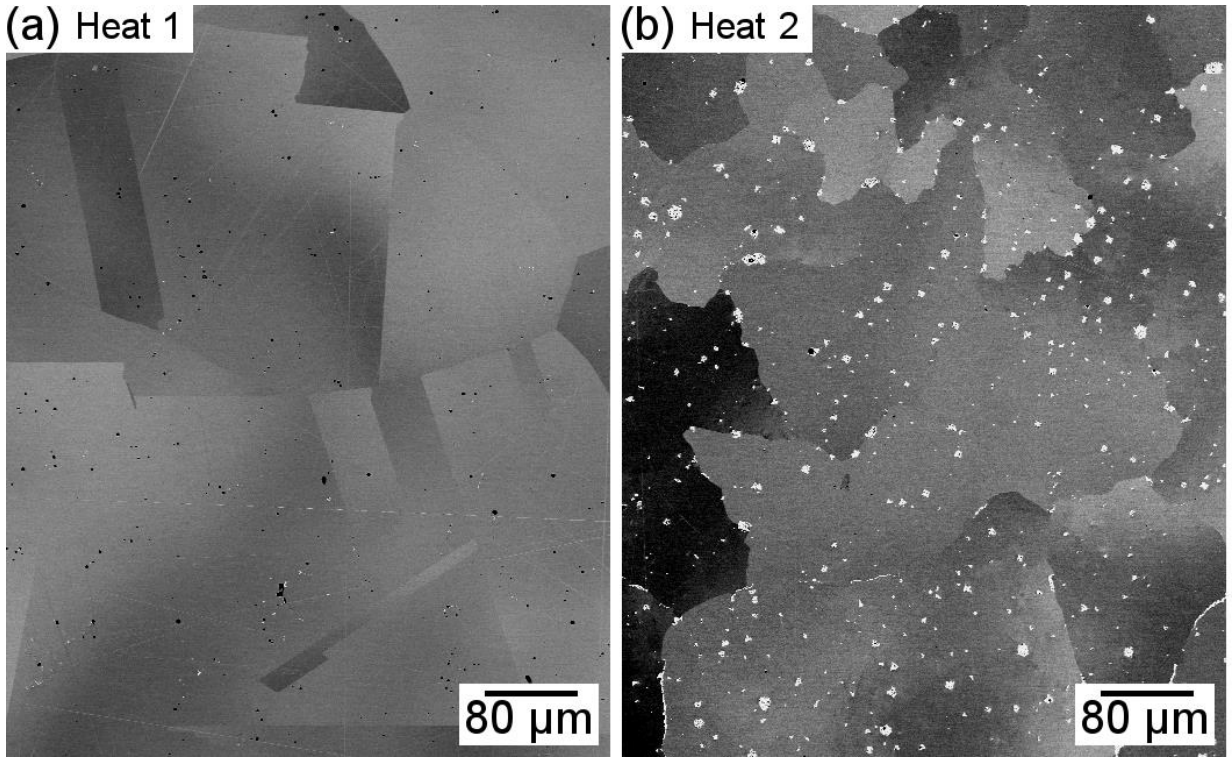

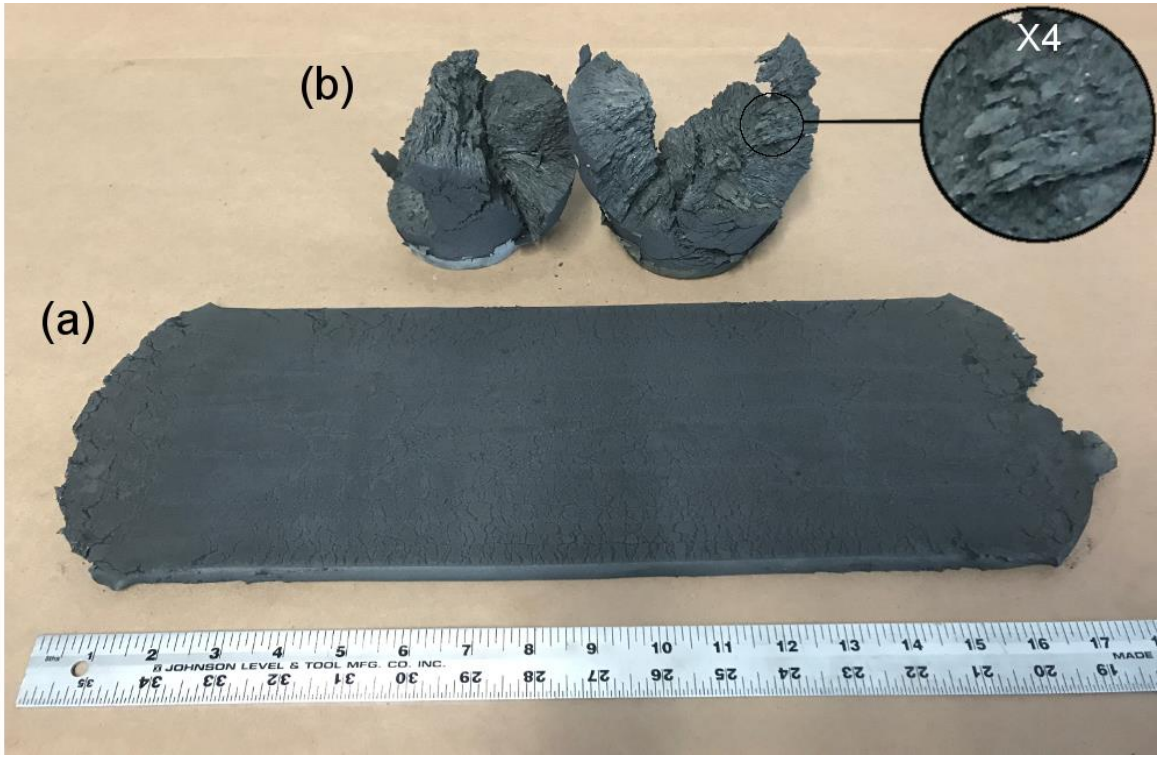

Remnant eutectic phase acted as preferential sites for stress concentration which induced cracking along the grain boundaries during deformation

Undesirable phases

Melting and Forging

(a) Failure along the grain boundaries in both equiaxed and columnar zones

(b) Evidence of crack propagation along a grain boundary containing the eutectic constituent

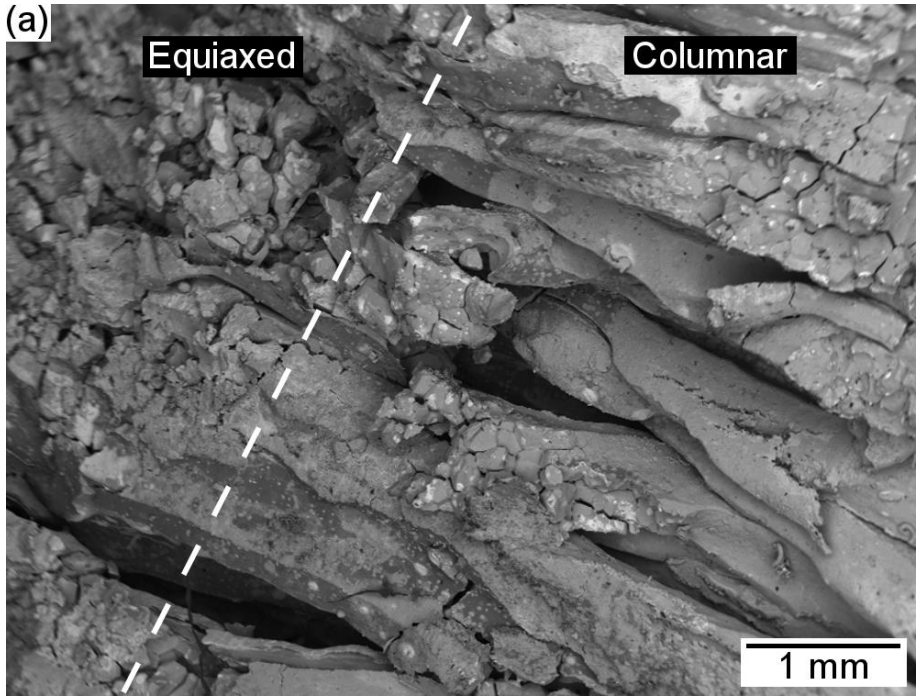

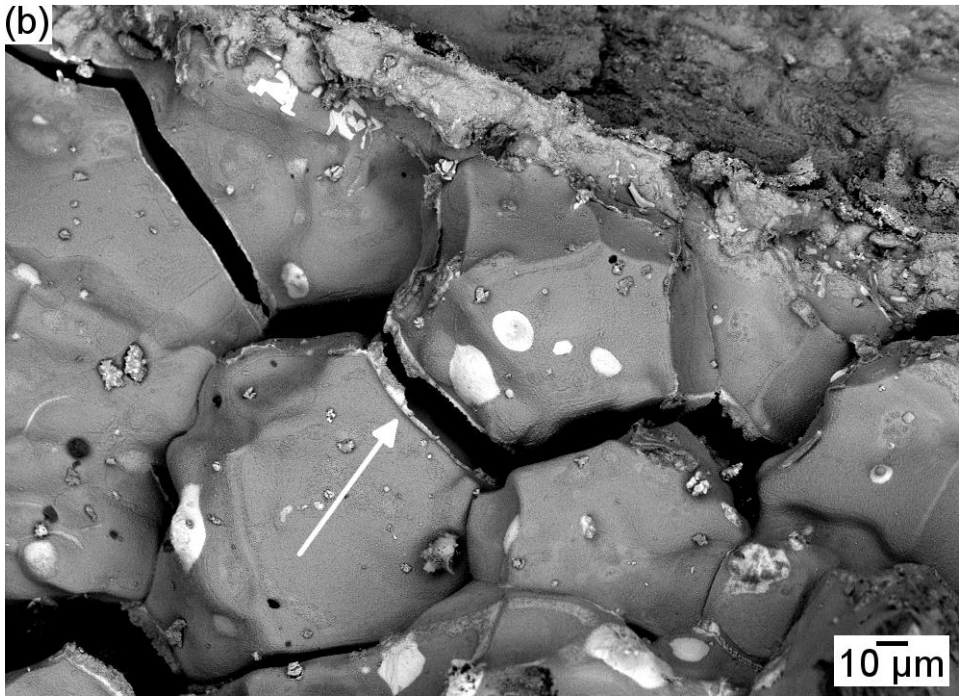

Conclusions

- Ni-based superalloys with the coexistence of γ' precipitation strengthening and high entropy γ matrix (defined by $\Delta S_{conf(matrix)}$>1.5R) in a temperature range that encompass operating temperatures suited for high-temperature applications.
- The ASC alloys exhibit superior yield stress when compared to a commercial Ni-based superalloy Nimonic 105 that contains a similar level of alloying. The microstructure consists of nano-sized γ' precipitates distributed within a FCC γ matrix. MC and grain boundary $M_{23}C_6$ carbides are present in the microstructure following aging.
- Deformation at high temperatures (1130 to 1210°C) and 0.001 s^{-1} resulted in a near-superplastic flow mechanism with limited flow hardening leading to the formation of a sub-structure within the grains.
- Temperatures from 1170 to 1210°C and strain rates from 0.01 to 0.1 s^{-1} led to recrystallized microstructures through DDRX with finer grain sizes compared to the starting conditions.
- Dislocation-based plastic behavior leading to partially recrystallized microstructures resulted from deformation at or below 1130°C (at the exception of 1130°C – 0.001 s^{-1}). The microstructures consisted of large deformed grains with a necklace structure of fine recrystallized grains around their boundaries.
- Significant variations in flow behavior affected the accuracy of the flow stress model. The model can be used to identify regions of different flow mechanisms which allows for the calculation of the activation energy and material constants for each deformation mechanism.
- Benefit of high entropy γ matrix? (to significantly change the matrix entropy it is necessary to make compositional changes that lead to changes in precipitation behavior)

Acknowledgment

This work was performed, in part, in support of the US Department of Energy's Fossil Energy Crosscutting Technology Research Program. The Research was executed through the NETL Research and Innovation Center's Advanced Alloy Development Field Work Proposal. Research performed by Leidos Research Support Team staff was conducted under the RSS contract 89243318CFE000003. MD, PDJ and JAH would like to thank Mr. Edward Argetsinger (NETL/USSE2) and Mr. Joseph Mendenhall (NETL/USSE2) for assistance in melting and Mr. Christopher Powell (NETL/USSE2) for tensile testing. SA would like to acknowledge the funding from the Natural National Science Foundation of China [grant No. 51850410518] and the China Postdoctoral Science Foundation [grant No. 2018M630069]. MD and ST would like to thank Dr. Joshua McCarley (IIT) for Gleeble testing.

Disclaimer

This work was funded, in part, by the Department of Energy, National Energy Technology Laboratory, an agency of the United States Government, through a support contract with Leidos Research Support Team (LRST). Neither the United States Government nor any agency thereof, nor any of their employees, nor LRST, nor any of their employees, makes any warranty, expressed or implied, or assumes any legal liability or responsibility for the accuracy, completeness, or usefulness of any information, apparatus, product, or process disclosed, or represents that its use would not infringe privately owned rights. Reference herein to any specific commercial product, process, or service by trade name, trademark, manufacturer, or otherwise, does not necessarily constitute or imply its endorsement, recommendation, or favoring by the United States Government or any agency thereof. The views and opinions of authors expressed herein do not necessarily state or reflect those of the United States Government or any agency thereof.